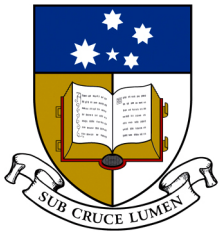

Tectonic Evolution of the Far Western and Northern Gawler Craton

Samuel W. Deed

Continental Evolution Research Group, Discipline of Geology and Geophysics,
School of Earth & Environmental Sciences
The University of Adelaide, Adelaide, Australia

Supervisors: **Assoc. Prof. Martin Hand**
Dr Karin Barovich
Katie Howard

Table of Contents

List of Figures

List of Tables

Tectonic Evolution of the Far Western and Northern Gawler Craton

Samuel W. Deed

Continental Evolution Research Group, School of Earth & Environmental Sciences, The University of Adelaide, Adelaide, Australia

Abstract

The Gawler Craton is an extensive region of Archaean to Mesoproterozoic crystalline basement underlying approximately 440 000 km^2 of central South Australia that has seen extensive tectonothermal events. The tectonics of the region are particularly important in both mineral exploration and Palaeoproterozoic reconstruction models. A potential key to the understanding of both is the Nawa Domain which ties the Late Archaean-Early Palaeoproterozoic core of the Gawler Craton to the Mesoproterozoic Musgrave Province. The Nawa Domain covers an area of approximately 150,000 km^2 on the northern edge of the Gawler Craton. Despite extensive geological exploration throughout, little is known of the significant geological history and formation of the region. An understanding of the evolution and tectonic history of the Nawa Domain as a part of the Gawler Craton could provide significant insight into establishing future economic prospects and would have particular importance in Palaeoproterozoic reconstruction models. The significant tectonic history and geology of the Gawler Craton has been examined and described over the following durations, the Archaean, Paleoproterozoic, and the Mesoproterozoic. It should be noted that in this duration the Gawler Craton records the effects of at least 7 regional-scale tectonothermal events. Recent studies have indicated that of these tectonothermal events, the Kimban has particular significance in the western and northern Gawler Craton which is reflected in the results of this study with zircon and monazite ages as reflecting Kimban aged

deformation. This study focuses on application of U-Pb LA-ICP-MS zircon and monazite geochronology to constrain the timing of deformation of metamorphism in the northern Gawler Craton with microprobe analysis defining peak metamorphic conditions.

Keywords: *Tectonic, Gawler Craton, LA-ICP-MS, Nawa, LA-ICP-MS.*

1 Introduction

Numerous tectonic events are known to have occurred across the Gawler Craton at different times with varying degrees of deformation seen regionally (Daly et al., 1998; Fanning et al., 2007; Hand et al., 2007). The significance of these events has implications in topics such as Palaeoproterozoic reconstructions models of Australia and effective mineral exploration strategies in complex basement terrains. The Gawler Craton is host to an extensive list of prospective commodities such as Cu, Au, Ni, Ag, Pb, Zn, U, Pt, Pd, REE, Sn, Cr, and iron ore. It hosts deposits such as Olympic Dam which is known for its Cu-Au-U-REE deposits. This single deposit is responsible for ~40 percent of the world's known uranium resources as well as world-class resources of Cu and Au (Hand et al., 2007). The mineralisation at Olympic Dam is temporally and spatially associated with a major tectonic/tectonothermal event, the Hiltaba Suite/Gawler Range Volcanic magmatic event which occurred ~1595-1575 Ma (Daly et al., 1998; Hand et al., 2007). An understanding of the evolution and tectonic history of the craton could help establish future economic prospects.

Reconstruction models attempting to describe the evolution of the Gawler Craton have been limited by the distinct absence of outcrop exposure over significantly large areas of the craton. Over the last 10-15 years, the acquisition and

interpretation of regional-scale geophysical datasets in addition to drilling has allowed appraisal of poorly to non exposed regions of the craton (Fairclough and Daly, 1995; Daly et al., 1998; Direen et al., 2002; Betts et al., 2003; Direen et al., 2005; Hand et al., 2007). On a larger scale, reconstruction models for the Proterozoic North Australian Craton (NAC) and the SAC (South Australian Craton) have focussed heavily on the interaction of the Gawler Craton and the NAC with the Musgrave Province (Myers et al. 1996; Karlstrom et al. 2001; Betts et al. 2002; Dawson et al. 2002; Giles et al., 2002, 2004; Fitzsimons 2003; Betts & Giles 2006; Schmidt et al. 2006; Wade et al., 2006). Key to these arguments are the geological constraints in key regions (Payne et al., 2008) such as the Nawa Domain. The Nawa Domain is situated in the western and northern end of the Gawler and is the link between the Late Archaean-Early Palaeoproterozoic core of the Gawler Craton and the Mesoproterozoic Musgrave Province (Payne et al., 2008). Despite the relative importance of the Nawa Domain either for economic interest or continental terrain reconstructions, very little is known about the tectonic events that define the region and shaped the underlying crystalline basement.

1.1 Geological Background

The Gawler Craton sits within the South Australian Craton and is an extensive region of Archaean to Mesoproterozoic crystalline basement underlying approximately 440 000 km^2 of central South Australia (Daly et al., 1998) (Figure 1). It is an oval shaped craton with dimensions 800 x 600 km and is centred upon the Gawler Ranges. The region has remained a stable platform except for local epeirogenic movements (uplift or depression of the earth's crust, affecting large areas of land) since approximately

1450 Ma (Fanning et al., 2007). Primary Industries and Resources SA (PIRSA) indicate that the boundaries of the craton are defined to the northeast, northwest and west by faulted margins and thick Neoproterozoic and Phanerozoic sedimentary basins. To the east and southeast the Torrens Hinge Zone (THZ) defines the margin, adjacent to the western limit of the Adelaide Fold Belt. The southern boundary is coincident with the edge of the continental shelf. Much of the area is covered by thin platformal sediments and regolith covering of Neoproterozoic to Cainozoic age. The basement of the Gawler Craton was formed during the Late Archaean (2560-2500 Ma) and the Paleoproterozoic (c.2000-1850 Ma). The basement rocks are intruded and overlain by Late Paleoproterozoic (1750-1600 Ma) to early Mesoproterozoic (1600-1550 Ma) rocks (Daly et al., 1998; Swain et al., 2005; Hand et al., 2007).

Previously, the tectonics that occurred across the craton have been studied and the existence of three orogenies with another tectonic key event, maybe two, have been proposed (Drexel, 1993; Daly, 1998). Different studies of the Craton generate differing perspectives. This is made rather evident in a study by Hand et al., (2007) where three previous works are considered and their proposed key events and age relationships of the events compared and contrasted with his own and numerous others results. It is highlighted that the Gawler Craton preserves the effects of at least seven regional-scale tectonothermal events across the craton and provides a comparison between the nomenclature framework as suggested in Hand et al. (2007) and previous terminology for the tectonic events in the Gawler craton (Drexel, 1993; Daly, 1998).

Ultimately, models attempting to describe the evolution of the Gawler Craton have been limited by the distinct absence of outcrop exposure over significantly large areas of the craton. Over the last 10-15 years, the acquisition and interpretation of

regional-scale geophysical datasets in addition to drilling has allowed appraisal of poorly to non-exposed regions of the craton (Fairclough and Daly, 1995; Daly et al., 1998; Direen et al., 2002; Betts et al., 2003; Direen et al., 2005; Hand et al., 2007).

The evolution of the Gawler is still not very well understood. Current research indicates there to have been at least seven key tectonic events that shaped the evolution of the Gawler Craton (Hand et al., 2007). The oldest event was the Sleafordian Orogeny which likely occurred at around 2480-2420 Ma. The early Palaeoproterozoic Sleafordian Orogeny (Daly and Fanning, 1993; Daly et al., 1998) terminated the late Archaean basin evolution and volcanism (Hand et al. 2007). Prograde mineral assemblages in the Carnot Gneisses record granulite facies metamorphism during the Sleafordian Orogeny. The central part of the craton equilibration temperatures attained 800-860°C at pressures of approximately 9 kbar (Fanning et al. 1986). Rb-Sr and U-Pb geochronology indicates a peak metamorphic age of ca. 2440 Ma (Fanning et al., 2007). Lower metamorphic grades in the southern part of the craton are characterised by andalusite-chloritoid-bearing assemblages (Schwarz, 2003). At around ca. 2000 Ma, the Miltalie Event is poorly characterised and was followed by the Cornian Orogeny at around 1850 Ma. The broad expression of the Cornian Orogeny is obscured by the later Kimban Orogeny and also by the 1760 Ma Wallaroo Group, which unconformably overlies rocks affected by the Cornian Orogeny (Zang et al., 2002; Hand et al., 2007). It appears likely that the Cornian event was a major tectonic event in the eastern Gawler Craton. The Kimban Orogeny occurred at around 1730-1680 and was widespread. It consisted of three tectonic events (Parker, 1993b). Within the eastern region of the Gawler, the most obvious expression of tectonism is the Kalinjala Shear system which forms a subvertical high-strain zone between 4 and 6 km wide along the eastern of Eyre

Peninsula (Parker et al., 1993; Vassallo and Wilson, 2001, 2002; Tong et al., 2004; Swain et al., 2005b). Macroscopic drag into the shear zone indicates that it formed during dextral shear (Vassallo and Wilson, 2002), giving an indication that the Kimban Orogen was a dextrally transpressive system. Granulitic lower crustal rocks can be found within the shear zone are derived from the Donington suite. These rocks have been exhumed from ~35 km depth along steeply decompressional paths, and juxtaposed against mid crustal rocks on the shear zone flanks (Parker, 1980; Hand et al., 1996). From data collected using Sensitive High Resolution Ion Microprobe (SHRIMP) zircon U-Pb, Sm-Nd garnet and monazite U-Th-Pb ages from the shear fabrics (Hand et al., 1996) there is suggestion that the shear system formed over the interval ~1730-1680 Ma (Hand et al., 2007). Terrain-scale shear systems in the western Gawler Craton reworked the granulites that formed during the Sleafordian Orogeny (Swain et al., 2005b). These shear zones have medium pressure Barrovian assemblages (Teasdale, 1997; Thomas, 2004) and record dextral transport. From within the shear system, Monazite Th-U-Pb ages were obtained from mylonites. These ages of around 1685 Ma (Swain et al. 2005b), indicate that the shear systems were active during the Kimban Orogeny. Granites belonging to the 1690-1670 Ma Tunkillia Suite (Ferris et al., 2002) appear in part synchronous with deformation on the shear zone systems (Swain et al., 2005b).

The deformation and metamorphism of the more recent tectonic events are poorly constrained and hence, they are listed as the Ooldean Event (1660-1640 Ma), Nawan Event (1620-1600 Ma), Hiltaba Event (1595-1570 Ma), Kararan Orogeny (c.1560-1540 Ma), and regional-scale shear zone reactivation (1470-1450 Ma).

The Gawler Craton has been divided up into 14 tectonic domains (Ferris et al. 2002) that are distinct and characterised by total magnetic intensity (TMI), gravity

datasets, and limited geological evidence (Payne et al., 2008). These domains are typically partitioned by crustal scale shear zones and faults. This study focuses on the Nawa Domain which lies on the north western edge of the Gawler Craton and trends north east (Figure 1). All the samples collected in this study originate from the Nawa Domain (Figure 1) which represents ~150 000 km^2 of the Northern Gawler Craton (Payne et al., 2006). The region generally contains both metasediments and metaigneous rocks too. The timing of deposition of the Nawa metasedimentary rocks is unknown (Payne et al., 2006).

2 Methods

The samples that were obtained for this study were cut from quarter core obtained from PIRSA's Drill Core Storage Facility located in Glenside, S.A. The samples were generally homogenous and were selected on the basis that they best represented the surrounding depth. Due to limitations on each of the sampled drill holes and the quantity of core available, only minor quantities of the sampled core was processed for whole-rock geochemistry and isotopic rock analysis. An aliquot of each sample was milled to a very fine powder by ball mill and then put aside for whole-rock geochemistry externally by Amdel Limited. The remaining sample was crushed by jaw crusher and then sieved, collecting the 79-300 μm portion. Zircon separates were obtained using panning and heavy liquid methods before being hand picked and mounted into epoxy resin blocks. The zircon grains were individually imaged at Adelaide Microscopy using Cathode-Luminescence (CL) imaging on a Phillips XL-20 SEM with attached Gatan Cathode-Luminescence analyser. Age dating using LA-ICP-MS (Laser Ablation Inductively Couped Plasma Mass Spectrometer) was conducted using two different methods, the first being single grain U-Pb isotopic

analysis of zircon which was conducted at both Macquarie University (GEMOC) and Adelaide by similar configurations. The second method was in-situ monazite dating targeting individual monazites in thin section. The LA-ICP-MS configuration consisted of a New Wave UP213 213 nm Nd-Yag Q-switching laser with attachment on spectroscope in a He ablation atmosphere, coupled to an Agilent 7500cs ICP-MS. In the first method the laser pit diameter was 40 μm, with a typical total depth of 40-50 μm. U-Pb fractionation was corrected at both Macquarie University and Adelaide University using the GEMOC 'GJ' zircon (TIMS normalisation data $^{207}Pb/^{206}Pb$ = 608.3 Ma, $^{206}Pb/^{238}U$ = 600.7 Ma and $^{207}Pb/^{235}U$ = 602.2 Ma, Jackson et al., 2004). Accuracy at Macquarie was checked with in-house '91500' (Wiedenbeck et al., 1995) and 'Mud Tank' standards (Black and Gulson, 1978), while at Adelaide the '91500' and the 'BJWP-1' (ca. 727 Ma) were used. Due to the significantly "old" zircon population the $^{207}Pb/^{206}Pb$ grain ages were used. A number of zircon grains were excluded from analysis due to metamict cores, minimal size, and complex lead laden cracks and fissures. Zircon cores larger than 40 μm in size were targeted, as well as some large metamorphic rims. In the data interpretation, a <10% discordancy threshold was used for all grains analysed. The method for this procedure was that a 60 second gas blank was analysed followed by 120 seconds of measurement during zircon ablation. Prior to each ablation, the laser was fired for 10 seconds with the shutter closed to allow beam stabilisation. The diameter of the beam was ~40 μm at the sample surface with a frequency of 5 Hz and an intensity of ~95%. The isotopes measured were ^{204}Pb, ^{206}Pb, ^{207}Pb, ^{208}Pb, ^{232}Th, and ^{238}U for 10, 15, 30, 10, 10, 15 ms respectively.

Sm-Nd isotope analyses were conducted at the University of Adelaide. Samples were spiked with a $^{150}Nd/^{147}Sm$ solution. HF was added to the sample

in Teflon ‘bombs’ and evaporated. The samples were then oven-heated at 190 °C for 5 days in HF in sealed Teflon bombs. The HF was then evaporated, with HNO_3 added shortly before samples were completely dry. Six molar HCl was added and samples were heated for 2 days at 160 °C. REE were separated in Biorad polyprep columns, this was then further separated in HDEHP impregnated Teflon-powder columns to isolate Sm and Nd. Nd was run on a Finnigan MAT 262 Thermal Ionisation Mass Spectrometer (TIMS) and Sm was run on a MAT 261 TIMS.

In addition to the above mentioned zircon age dating, in-situ monazite dating was conducted by LA-ICP-MS. The setup for this procedure was as described above for the zircon age dating and was conducted at Adelaide Microscopy except that monazite grains were targeted in-situ in thin section profile as opposed to hand picked and mounted in epoxy. The method for this procedure was that a 40 second gas blank was analysed followed by 40 seconds of measurement during in-situ monazite ablation. Prior to each ablation, the laser was fired for 10 seconds with the shutter closed to allow beam stabilisation. The diameter of the beam was ~8 μm at the sample surface with a frequency of 5 Hz and an intensity of ~65%. The isotopes measured were ^{204}Pb, ^{206}Pb, ^{207}Pb, and ^{238}U for 20, 30, 60, 30 ms respectively. U-Pb fractionation was corrected using the ‘MAdel’ monazite standard (TIMS normalisation data: $^{207}Pb/^{206}Pb$ = 490.7 Ma, $^{206}Pb/^{238}U$ = 514.8 Ma and $^{207}Pb/^{235}U$ = 510.4 Ma). Corrected age accuracy was confirmed prior to unknown analysis and throughout analysis runs by regular analyses of an in-house monazite standard, ‘222’ (TIMS normalization data: $^{207}Pb/^{206}Pb$ = 440-470 Ma, $^{206}Pb/^{238}U$ = 444-460 Ma and $^{207}Pb/^{235}U$ = 444-460 Ma).

The final stage of the project required conducting PT work to constrain the PT conditions of the rocks. This was carried out by conducting thermobarometry on

selected samples to determine the mineral compositions. Mineral compositions for the selected samples were obtained using a Cameca SX51 Electron Microprobe at Adelaide Microscopy, located at the University of Adelaide. The analyses were obtained using wavelength dispersive spectrometers. Quantitative analyses were run at an accelerating voltage of 15 kV and a beam current of 20 nA, with a beam diameter of 2-3 μm. Representative mineral compositions are given in Table 4.

3 Observations and results

3.1 Drill hole logs

The following drill hole descriptions are based on stratigraphic logs obtained from the South Australian Information Geoserver (SARIG) and the major units and relevant depths are listed in Table 5. Specific information regarding of selected samples in regards to depths and petrology is included in Table 6. The basement intersections were of primary interest in this study with no sampling conducted above the basement contacts.

3.1.1 Drill hole OBD 1

The OBD 1 drill hole was drilled to a depth of 140 meters and contacted basement at 115.3m. The first unit was precollar and was not collected. The second unit was described as undifferentiated Carboniferous-Permian age rock that throughout the retained drill core were found to contain fragments of basement. The basement that was seen in OBD 1 was a granitic gneiss comprising quartz, feldspar, biotite, garnet with veins of haematite and calcite. A mineral assemblage of garnet – orthopyroxene

– plagioclase – biotite – opaque mineral – clinopyroxene was typically seen in OBD 1.

3.1.2 Drill hole OBD 3

The OBD 3 drill hole was drilled to a depth of 218m and contacted basement at 123m. The first unit is an Oligocene silicified conglomerate of aoelian red sands, red clays, and red ferruginous sandstone. The second unit was described as Eocene to Quaternary undifferentiated silcrete. The third unit was a red-brown fine to coarse-grained sandstone unit with granule and pebbled layers and shale intraclasts. The fourth unit was another sandstone-siltstone unit. It was described as a diamictite with shale intercalations in the basal unit with the upper unit being rhythmically bedded coarse and fine-grained clastics. Subaqueous deposition of glacial debris transported was apparently seen as mud flows. The basement unit was contacted at 123m and is described as undifferentiated Palaeo-Mesoproterozoic medium-coarse grain, partly gneissic and chloritic granite. Towards its top is a conglomerate layer comprising granitic pebbles. The assemblage was seen to be plagioclase – quartz – biotite(altered) – hornblende (mostly altered) – opaque mineral.

3.1.3 Drill hole OBD 5

The OBD 5 drill hole was drilled to a depth of 134.1m and contacted basement at 131.8m. Three major units were intersected by this drill hole. The first unit was rotary precollar and was not collected. The second unit was typically made up of siltstone and mudstone. It was described as being a brown-green siltstone/mudstone and claystone with occasional basement fragments, micacaeous, calcareous and dolomitic

in part with minor sandstone, limestone, and chert. At the contact between basement and this second unit the contact is defined by a grey-green (occasionally brown) calcareous conglomerate with fragments mostly limestone with some gneissic granite basement fragments. The third unit was basement which was granite. Only one sample was collected from the basement, its mineral assemblage is K-feldspar – quartz – plagioclase – hornblende (altered) – minor garnet – biotite (altered).

3.1.4 Drill hole OBD 7

The OBD 7 drill hole was drilled to a depth of 269.60m and includes a total exposure of 9.2m of granite basement. The first unit was precollar and was not collected. The second unit was an undifferentiated Carboniferous-Permian sandstone/siltstone with a conglomerate base. It was seen to be a white-pink sandstone with occasional basement fragments at the top while towards the bottom it becomes a poorly sorted grey-green siltstone that becomes increasingly conglomeratic towards the base. The third unit was another sandstone/siltstone with a conglomerate base. At the contact, there was a sharp thin layer of dark red ferruginous conglomerate with subrounded granite fragments up to 5mm in diameter. The basement contact seen in this drill hole was a pink feldspathic granite. A mineral assemblage of K-feldspar – plagioclase – biotite – quartz was seen in typically seen in OBD 7.

3.1.5 Drill hole OBD 8

The OBD 8 drill hole was drilled to a depth of 185m and contacted granite basement at 175.2m. The first unit was precollar with no sample collected. The second unit was a sandstone/siltstone unit with occasional basement fragments throughout which was

described as diamictite with shale intercalations in the basal unit with the upper unit rhythmically bedded with coarse and fine-grained clastics. Subaqueous deposition of glacial debris was transported as mud flows. The basement was seen to be a grey-pink medium grained granite with a mineral assemblage biotite – plagioclase – quartz – opaque mineral.

3.1.6 Drill hole OBD 9

The OBD 9 drill hole was drilled to a maximum depth of 400.7m and contacted basement at 389m. The first unit was precollar with no sample collected. The second unit was an undifferentiated Carboniferous-Permian sandstone/siltstone that was described as an unconsolidated conglomerate with granitic basement pebbles. Underlying this, the third unit was a grey-green siltstone/shale and claystone layer that was micacaeous, calcareous and dolomitic in part with minor sandstone, limestone, dolomite, and chert. Within its extent were layers of red-brown siltstone shale that were often laminated and calcareous in parts. The unit was a fine to medium grained sandstone with shale intraclasts. It ranged from a buff-green feldspathic sandstone to a buff-pink sandstone with red-brown siltstone laminations. The final unit was the basement which was a grey-white granitic gneiss with a typical assemblage of garnet –biotite – plagioclase – quartz – K-feldspar.

3.1.7 Drill hole OBD 11

The OBD 11 drill hole was drilled to a maximum depth of 232.7m with basement contacted at 223.7m. The first unit was an Oligocene silicified gritty conglomerate and sandstone. The second unit was a sandstone/siltstone. It was described as a buff-

brown carbonaceous sandstone/siltstone with organic material and minor lignite and trace pyrite. The third unit was a fine to medium-grained sandstone, feldspathic in parts, with shale intraclasts. At the top of the depth, 116-166m, it was pale green feldspathic sandstone while in the remaining component, 166-224m the rock was a red brown lithic sandstone. The basement found in this drill hole was a pink gneissic granite. Samples seen from this drill hole had mineral assemblages of hornblende – plagioclase – biotite – quartz – opaque mineral.

3.1.8 Drill hole OBD 12

The OBD 12 drill hole was drilled due to a failure of OBD 10 to intersect basement. The drill hole reached a maximum depth of 474.4m and contacted gneiss basement at 463.4m. The first unit was a sand unit, which was calcareous near the top. It contained an Oligocene silicified gritty conglomerate. The second unit was a dolomitic siltstone and claystone that was micacaeous, calcareous in part with minor sandstone, limestone, and chert. The third unit was a fine to medium-grained sandstone with shale intraclasts with trace pyrite. The final unit was the basement which was a grey green and pink quartz – feldspar – phlogopite gneiss.

3.1.9 Drill hole Lake Maurice East 1

The Lake Maurice East 1 drill hole was drilled to a maximum depth of 722.38m and contacted basement at 691m. It was divided into the two key units, a sandstone layer and the underlying crystalline basement gneiss. The sandstone unit was described as a fine to medium-grained sandstone with shale intraclasts. The basement was recorded

to be a magnetite-rich aluminous metapelite, a metasediment. On inspection, it had a mylonitic assemblage of garnet – quartz – K-feldspar – plagioclase – opaque mineral and was extensively altered.

3.1.10 Drill hole Mount Furner 1

The Mount Furner 1 drill hole was drilled to a maximum depth of 555.04m with basement contact at 548.64m. The first unit was a shale siltstone that was described as being a grey, bioturbated, fossiliferous and shaly mudstone with minor silt to very fine-grained sandstone intervals. The Second unit was a medium to coarse-grained sandstone that is dolomitic towards the top. Unit three was a fine to medium-grained sandstone with granules and pebble layers, and with shale intraclasts while unit four was a sandstone siltstone interbedded with coal, shale and rare carbonate. The depositional environment was thought to include anoxic marine-lacustrine, deltaic changing up-section to lacustrine and fluvial. The fifth unit was a claystone with minor silt and sand which was described as shale with minor siltstone and sandstone deposited in a quiet water restricted marine environment. The basement seen in this drillcore was gneiss. It was a well banded garnet – sillimanite – biotite – plagioclase – quartz gneiss.

3.1.11 Drill hole Manya 4

The Manya 4 drill hole was drilled to an extent of 806.7m and contacted basement at 796m. The first four units are an undifferentiated Tertiary to Pleistocene silcrete, a weathered claystone/mudstone grading down to medium-grained quartzose

moderately sorted sandstone, a fine to coarse-grained sandstone, and another sandstone/claystone that is very fine to coarse-grained, quartzose and well sorted angular sandstone. The fifth, sixth, and seventh units were listed as a shale with minor claystone diamictite, dolomotic rock with minor siltstone that was fine to coarse-grained with minor sandstone, and another sandstone layer that is red-brown to green. The basement was seen to be a gneiss and was described as an undifferentiated Palaeoproterozoic rock, a gneiss to micaceous schist with banded vein filling. It had a typical mineral assemblage of garnet – biotite – K-feldspar – quartz – plagioclase.

3.1.12 Drill Hole Middle Bore 1

The Middle Bore drill hole was drilled to a maximum depth of 557.60m and contacted basement at 371.0m. The first unit was a multicoloured claystone silicified to six metres. The second unit was a clayey to very coarse grained subangular to subrounded poorly sorted sandstone that was interbedded with coal, shale, are rare carbonates. The third unit was mixed carbonates/siliclastics with minor dolomite, marine carbonates and evaporites. The basement was a brecciated gneiss over gneiss and granulite with biotite – garnet – phlogopite – pyroxene – quartz – talc and some calcite and chlorite.

3.2 Zircon U-Pb results

Seven drill holes were examined, sampled, and analysed for zircon U-Pb ages. The seven drill holes were: OBD 1, OBD 3, OBD 5, OBD 6, OBD 8, OBD 11, and Middle Bore 1. The isotopic analyses focused on $^{207}Pb/^{206}Pb$ age spectra as this was most

likely to represent realistic age based analyses when looking at ages in excess of 1 Ga. (Eckelmann and Kulp, 1956). The resulting age spectra are presented in Figure 9 in the form of mean weighted histograms and density plots indicating relative abundance of zircon ages. Another author that looked extensively into the same region of the Gawler Craton (Payne et al. 2006), remarked that due to the relatively limited availability of drill core, the number of zircon grains that could be separated, in most cases, was below the recommended numbers for detrital zircon studies (Vermeesch, 2004; Andersen, 2005). An example of the statistically significant results as discussed by Vermeesch (2004) is that in order to be 95% confident that no fraction ≥0.05 was missed of one age population, at least k=117 grains must be dated. This condition was not met is this study due to availability of zircons and time constraints.

As seen in Figure 9 and reflected in the results of Payne at el., (2006), the dominant peaks occur over the intervals of 1740–1840 Ma. Peaks in the spectra are observed at 1730–1750, 1750–1780 and 1800–1820 Ma with lesser peaks at ca. 1900, 2050 and 2500 Ma.

3.3 Sm-Nd isotopes

Sm-Nd isotopic data for rocks of the Nawa Domain are tabulated in Table 2. Figure 6 displays a εNd Versus time diagram while Figure 12 is a REE plot comparing rocks of the Nawa against the Post-Archaean Australian Shale (PAAS). Figure 12, displays Chondrite-normalised REE patterns that have been normalized to average continental crust (Taylor and McLennan, 1985).

3.4 Monazite U-Pb results

Three drill holes were targeted for in-situ monazite age dating. Figure 7 shows representative monazite Back Scatter Electron (BSE) images. From these images it can be seen that not only is there significant variation in size and shape of monazites but degrees of compositional banding or zonation as well. It should be noted that within the monazites, the compositional banding that is seen in the BSE images did not seem to have any impact on the age of metamorphism within the monazite. An example of this is monazite 'e' in Figure 7. This particular monazite records a metamorphic history from 1717 +/- 19.8 Ma through to 1548.1 +/- 19.6 Ma. Distinct patches of light and dark are clearly evident in the image but they seem to be of no discernable impact on the specific age of the surrounding monazite. The sizes of monazite ranged from 15-20 μm up to hundreds of microns and were clearly visible in thin section in plain eyesight.

4 Discussion

The Nawa Domain is characterized by longer wavelength, lower amplitude magnetic anomalies (Direen et al., 2005), which are due to the thicker cover of the early Palaeozoic sediments of the Officer Basin as can be seen in Figure 2. The influence of these overlying Palaeozoic sediments is thought to be masking the magnetic effect of the underlying Paleoproterozoic magnetite-rich metasedimentary gneisses (Daly et al., 1998). Gravity data show that the Nawa Domain is a relative gravity high which is likely due to the presence of dense, high pressure rocks, including unusual quartz-sapphirine, hypersthene-sillimanite-quartz and spinel-sillimanite-quartz, garnet and hypersthene-sillimanite bearing, aluminous granulites encountered in drill holes (Rankin et al., 1989; Teasdale, 1997; Direen et al., 2005).

Payne et al. (2005) indicates that the constraints on the maximum age of deposition of the Nawa Domain metasedimentary rocks (NDM) is ~1740 Ma as is indicated by the youngest zircon grouping interpreted as detritals. He also noted that during his sampling, a distinct absence of older zircons, Archaean in age, in lithologies displaying evolved Nd isotopic signatures. This was typical of the sampling conducted in his study where he looked primarily at metasediments and strengthens his suggestion that there has been extensive intra-crustal recycling in the source regions. The evidence he uses for this is a significant negative Eu anomaly which is often interpreted to signify crustal re-working (McLennan and Taylor, 1988). The results of the sampling conducted in this study also reflect that a majority on the sampled drill holes contain significant Eu anomalies. An interesting result was seen in Figure 6 where it was noted that Middle Bore plotted with a value of ƐNd(T) = 3.3-3.5. This indicates that it has a more juvenile origin than the other drill holes which all plot negatively. From what was seen in the zircons from Middle Bore, Middle Bore 1 is a metaigneous rock. The drill hole itself sits in a large shear zone and the origin of the metaigneous rock could be explained by this fact. In Figure 6, there are two rectangles, one plots at ~1.6 Ga and the other ~1.7 Ga, they reflect the geochemical findings of Howard et al., (2006) and Payne et al., (2006). Both authors have sampled from the Gawler, with the results of Payne et al., (2006) collected in the Northern and Western Gawler while the results of Howard et al., (2006) collected from the Eastern Gawler. As their results and the geochemical findings of this study track together through time with overlapping values of ƐNd depletion this indicates suggests they have similar source regions.

The drill holes observed in the study record the mineral assemblages of reasonable high temperature low temperature granulites and under the P-T conditions

that these samples experienced it is thought that the monazite will record metamorphic ages (Parrish 1990; Rubatto et al., 2001; Kelsey et al. 2006). What was noted of interest from the monazite age dating was that the monazite generally seemed to reflect younger ages than ages obtained from zircon from the same drill hole and of the meterages. Payne et al., (2008) examined three of the same drill holes covered in this study, Mt Furner 1, Manya 4, Lake Maurice East 1, for monazite dating. His findings were that Mt Furner 1 likely had a single age distribution, as did Manya 4, and Lake Maurice East 1. His listed mean weighted $^{207}Pb/^{206}Pb$ ages are 1728 +/- 10 Ma, 1719.3 +/- 7.9 Ma, and 1713 +/- 9.5 Ma respectively.

4.1 PT Calculations

Pressure and temperature calculations were conducted using analyses obtained from the electron microprobe (Table 4). All samples chosen for analysis were garnet bearing. P-T calculations were conducted using the mineral core compositions in order to minimise the effects of retrograde resetting. Pressures and temperatures were calculated utilising the average-P and average-T approach (Powell & Holland 1994) using the computer program THERMOCALC v3.21 (Powell & Holland 1988) and the updated internally consistent dataset of Holland and Powell (1998).

The average P, average T, average P-T approaches are multiple equilibria techniques which utilise a least-squares method to calculate the optimal P-T conditions from the thermodynamic data of end-members involved in a series of independent reactions that entirely specify the thermodynamics of the system (Powell & Holland 1994). The average-P approach allows the calculation of pressure for a chosen temperature, while the average-T approach calculates the temperature for a

given pressure. The average-PT approach is the most powerful in estimating metamorphic conditions, calculating pressure and temperature simultaneously. This approach however, cannot always be used as some mineral assemblages or assemblage compositions may not allow an average-PT calculation due to an insensitivity to either pressure or temperature. In these cases, the average-P or average-T must be used. A number of samples from the northern Gawler Craton suffered from this limitation.

Compositions derived from the electron microprobe were recalculated using the program AX (Powell et al., 1998), which calculates the activities of the mineral end members. P-T calculations done with THERMOCALC include uncertainties on the mineral activities and enthalpies of mineral end-members, which are propagated through to the final results (Powell & Holland 1994). Each independent reaction is enclosed in an uncertainty envelope, the width of which plays a crucial role in determining the optimal P-T conditions. Thus a reaction with a large uncertainty envelope will contribute relatively little to the final result. As the reactions in the independent set involve overlapping subsets of end-members, the equilibria are constrained to move in a correlated way that results in the P-T intersection moving in a predictable manner. The results are subject to a χ^2 test. If this is passed, it means that a solution has been found that is consistent with input data and their uncertainties. These calculations allow the identification of end-members, which strongly influence the result as well as activities, which are not well fitted by the average result. Samples that fail the χ^2 tests will usually pass once outlying end-members have been identified and either omitted from the dataset or down played by increasing the uncertainty on their activities. The ability to identify end-members that either strongly influence the

results or are significant outliers means that the robustness of the P-T results and the degree of equilibrium between the chosen mineral compositions can be assessed.

Due to a comparatively limited range of mineral assemblages, some samples used in this study had ≤ 4 independent reactions utilised during the average P-T calculations.

A variable that is difficult to constrain using the average P-T approach is the behaviour of fluid. Since all the samples used in this study come from migmatitic or high-grade (opx-bearing) metamorphic rocks its likely that melt was present during metamorphism. However, specifying the activity of H_2O within the melt for each sample is beyond the scope of this study. Nevertheless calculations performed with a H_2O ranging between 0.25-0.5 did not significantly affect the results and $aH_2O = 0.25$ was used in all samples except Mt Furner 1 where muscovite-bearing migmatites probably had a higher aH_2O (White et al., 2003). In that case $aH_2O = 0.75$ was employed.

In samples that have a restricted mineral assemblage (e.g. Manya 4, OBD 3 and OBD 9), there are insufficient mineral endmembers to compute an average P-T result. In this case, garnet-biotite Fe-Mg thermometry was used to estimate a reference temperature which was then used to constrain an average pressure result.

5 Conclusion

From the results from the zircon and the monazite dating it is clear that that Kimban had a significant part to play in the history of these rocks which indicates that the influence of Kimban aged deformation was experienced widespread across the Gawler Craton. Most of the drill holes gave fairly clear evidence of Kimban ages with indications of younger tectonothermal events but more sampling would be required to better constrain the timings of these events. An interesting result was seen in OBD 9 where very few zircons were obtained from the drill hole but there was an abundance of monazite. From the Rare Earth and the εNd analyses it was noted that the drill holes of this study have similar geochemical properties to rocks of the Payne et al., (2006), in which case, this indicates that these rocks are likely derived from the sediments of the Arunta region.

Acknowledgements

I would like to acknowledge everyone who had a part in this thesis…
Angus Netting and the crowd from Adelaide Microscopy, David Bruce in the Isotope Lab, Anthony Reid from PIRSA, the gentlemen from PIRSA core storage facility, and to my girlfriend Alys who has help me put this together in the last days….
Finally, I would like to mention Brian Playford, he was a great mate and will be missed, my thoughts are with Amanda and his family.

References

Andersen, T., 2005. Detrital zircons as tracers of sedimentary provenance: limiting conditions from statistics and numerical simulation. Chem. Geol. 216 (3–4), 249–270.

Betts, P. G., Valenta, R. K., and Finlay, J., 2003, Evolution of the Mount Woods Inlier, northern Gawler Craton, southern Australia; an integrated structural and aeromagnetic analysis: Tectonophysics, v. 366, p. 83-111.

Betts, P. G., and Giles, D., 2006, The 1800-1100 Ma tectonic evolution of Australia: Precambrian Research, v. 144, p. 92–125.

Betts, P. G., Giles, D., Lister, G. S., and Frick, L. R., 2002, Evolution of the Australian lithosphere: Australian Journal of Earth Sciences, v. 49, p. 661–695.

Betts, P. G., Valenta, R. K., and Finlay, J., 2003, Evolution of the Mount Woods Inlier, northern Gawler Craton, southern Australia; an integrated structural and aeromagnetic analysis: Tectonophysics, v. 366, p. 83–111.

Blissett, A. H., Creaser, R. A., Daly, S., Flint, D. J., and Parker, A. J., 1993, Gawler Range Volcanics, in Drexel, J. F., Preiss, W. V., and Parker, A. J., eds., The Geology of South Australia. Vol 1. The Precambrian: South Australia. Geological Survey Bulletin 54, p. 107–131.

Creaser, R. A., and Cooper, J. A., 1993, U-Pb geochronology of middle Proterozoic felsic magmatism surrounding the Olympic Dam Cu-U-Au-Ag and Moonta Cu-Au-Ag deposits, South Australia: ECONOMIC GEOLOGY, v. 88, p. 186–197.

Daly, S. J., Fanning, C. M., and Fairclough, M. C., 1998, Tectonic evolution and exploration potential of the Gawler Craton, South Australia: AGSO Journal of Australian Geology and Geophysics, v. 17, p. 145–168.

Daly, S.J., and Fanning, C.M., 1993, Archean, in Drexel, J.F., Preiss, W.V., and Parker, A.J., eds., The Geology of South Australia; Volume 1, The Precambrian: South Australia Geological Survey, Bulletin 54, p. 32-49. (Have the Book at home).

Direen, N. G., Cadd, A. G., Lyons, P., and Teasdale, J. P., 2005, Architecture of Proterozoic shear zones in the Christie Domain, western Gawler Craton, Australia: Geophysical appraisal of a poorly exposed orogenic terrane: Precambrian Research, v. 142, p. 28–44.

Fanning, C. M., Flint, R. B., Parker, A. J., Ludwig, K. R., and Blissett, A. H., 1988, Refined Proterozoic evolution of the Gawler Craton, South Australia, through U-Pb zircon geochronology: Precambrian Research, v. 40-41, p. 363–386.

Fanning, C. M., Reid, A., and Teale, G., 2007, A geochronological framework for the Gawler Craton, South Australia: South Australia Geological Survey Bulletin 55, 258 p.

Ferris, G. M., and Schwarz, M. P., 2003, Proterozoic gold province of the central Gawler Craton: Minerals and Energy South Australia Journal, v. 30, p. 4–12.

Ferris, G. M., Schwarz, M. P., and Heithersay, P., 2002, The geological framework, distribution and controls of Fe-oxide and related alteration, and Cu-Au mineralisation in the Gawler Craton, South Australia. Part I: geological and tectonic framework, in Porter, T. M., ed., Hydrothermal Iron Oxide Copper-Gold and Related Deposits: a global perspective, 2: Adelaide, Porter Geoscience Consultancy Publishing, p. 9–31.

Fraser, G., and Lyons, P., 2006, Timing of Mesoproterozoic tectonic activity in the northwestern Gawler Craton constrained by 40Ar/39Ar geochronology: Precambrian Research, v. 151, p. 160–184.

Giles, D., Betts, P. G., and Lister, G. S., 2004, 1.8-1.5-Ga links between the North and South Australian Cratons and the Early-Middle Proterozoic configuration of Australia: Tectonophysics, v. 380, p. 27–41.

Hand, M., Reid, A, Jagodzinski, L., 2007, Tectonic Framework and Evolution of the Gawler Craton, Southern Australia. Society of Economic Geologists, Inc. Economic Geology, v. 102, pp.

Howard, K., Reid, A., Hand, M., Barovich, K., and Belousova, E. A., 2006, Does the Kalinjala Shear Zone represent a palaeo-suture zone? Implications for distribution of styles of Mesoproterozoic mineralisation in the Gawler Craton: Minerals and Energy South Australia Journal, v. 43, p. 6–11.

Jackson, S.E., Pearson, N.J., Griffin, W.L., Belousova, E.A., 2004. The application of laser ablation-inductively coupled plasma-mass spectrometry to in-situ U–Pb zircon geochronology. Chem. Geol. 211 (1–2), 47–69.

Johnson, J. P., and Cross, K. C., 1995, U-Pb geochronological constraints on the genesis of the Olympic Dam Cu-U-Au-Ag deposit, South Australia: ECONOMIC GEOLOGY, v. 90, p. 1046–1063.

Johnson, J. P., and McCulloch, M. T., 1995, Sources of mineralising fluids for the Olympic Dam Deposit (South Australia); Sm-Nd isotopic constraints: Chemical Geology, v. 121, p. 177–199.

Kelsey, D. E., Clark, C., and Hand, M., 2008, Thermobarometric modelling of zircon and monazite growth in melt-bearing systems: examples using model metapelitic and metapsammitic granulites. Journal of Metamorphic Geology, 26, 199-212.

Kelsey, D., Clark, C. & Hand, M., 2006. Integrating zircon and monazite saturation with metamorphism in melt-bearing systems. Geochimica et Cosmochimica Acta 70 (18, Supplement 1), A312.

McLean, M. A., and Betts, P. G., 2003, Geophysical constraints of shear zones and geometry of the Hiltaba Suite granites in the western Gawler Craton, Australia: Australian Journal of Earth Sciences, v. 50, p. 525–541.

Parker, A. J., and Lemon, N. M., 1982, Reconstruction of the early Proterozoic stratigraphy of the Gawler Craton, South Australia: Journal of the Geological Society of Australia, v. 29, p. 221–238.

Payne, J., Barovich, K., and Hand, M., 2006, Provenance of metasedimentary rocks in the northern Gawler Craton, Australia: Implications for Paleoproterozoic reconstructions: Precambrian Research, v. 148, p. 275–291.

Swain, G., Woodhouse, A., Hand, M., Barovich, K., Schwarz, M., and Fanning, C. M., 2005a, Provenance and tectonic development of the late Archaean Gawler Craton, Australia; U-Pb zircon, geochemical and Sm-Nd isotopic implications: Precambrian Research, v. 141, p. 106–136.

Swain, G., Hand, M., Teasdale, J., Rutherford, L., and Clark, C., 2005b, Age constraints on terrane-scale shear zones in the Gawler Craton, southern Australia: Precambrian Research, v. 139, p. 164–180.

Teasdale, J., 1997, Methods for understanding poorly exposed terranes: The interpretive geology and tectonothermal evolution of the western Gawler Craton, Unpublished Ph.D thesis, University of Adelaide.

Vassallo, J. J., and Wilson, C. J. L., 2002, Paleoproterozoic regional-scale non-coaxial deformation; an example from eastern Eyre Peninsula, South Australia: Journal of Structural Geology, v. 24, p. 1–24.

Vermeesch, P., 2004. How many grains are needed for a provenance study? Earth Planet. Sci. Lett. 224 (3–4), 441–451.

Figure Captions

Figure 1: This is a general outline of the Gawler Craton traced onto the coastline of south Australia. It indicates the position of the Nawa Domain in relation to the rest of the Gawler Craton.

Figure 2: These are all the drill holes looked at in this study plotted against a Total Magnetic Intensity image of the Nawa Domain

Figure 3: Selected petrograghy images from drill holes from Manya 4, Middle Bore 1, and Mt Furner 1.

Figure 4: Selected zircon CL images. Zircons on the Left, **a,** are Middle Bore 1 A metaigneous rock) while the zircons on the right, **b**, are from OBD 1 (a metasediment)

Figure 5: The Concordias of the selected zircons seen in CL in Figure 4

Figure 6: Epsilon Nd Vs Time plot.

Figure 7: Selected BSE images of Monazites.

Figure 8: All monazite Concordia data plotted by drill hole

Figure 9: Compilation of all zircon age data

Figure 10: Compilation of all metamorphic age data

Figure 11: REE plot geochem samples

Figure 12: PT results.

Figure 13: PT data.

Figure 1.

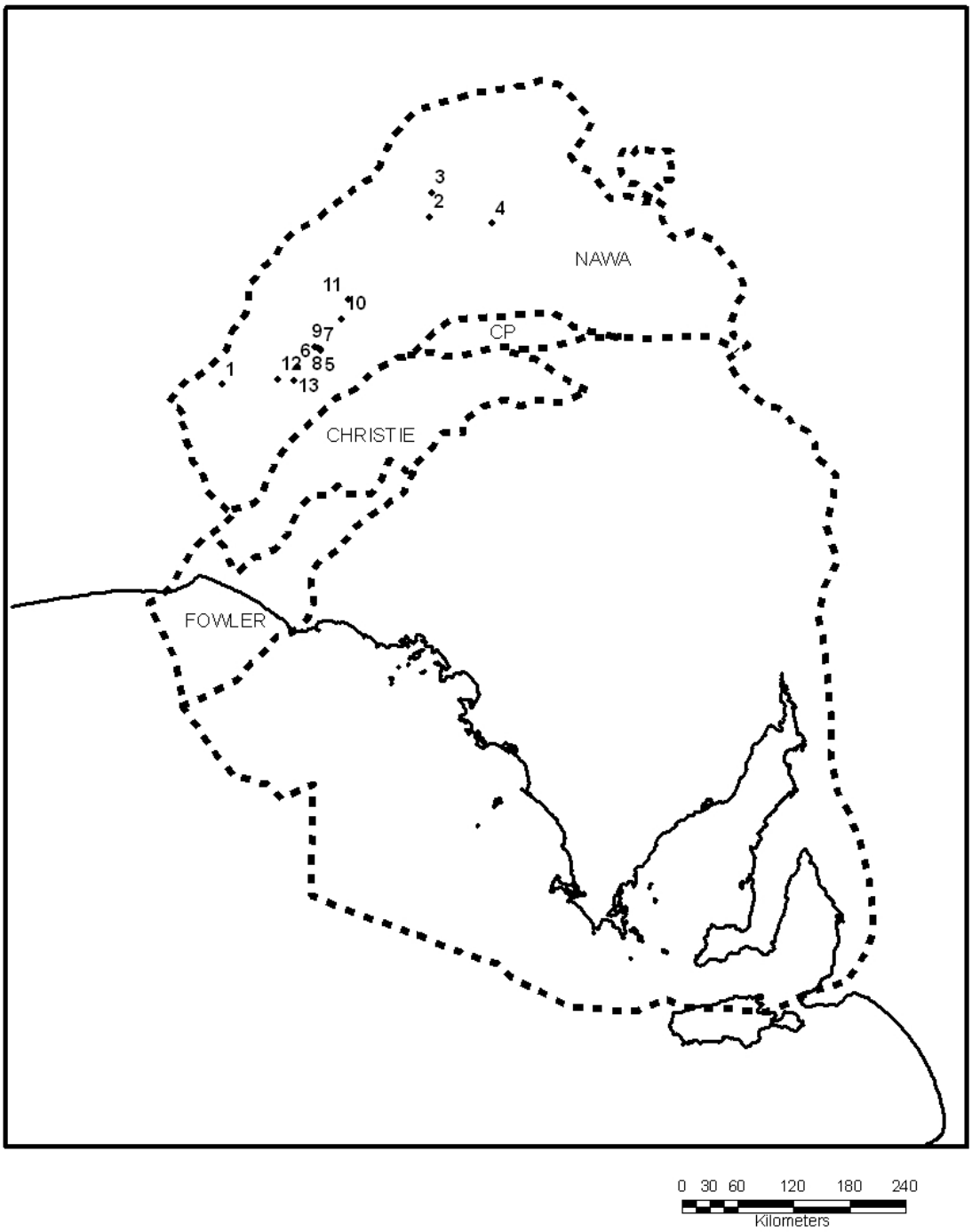
3
2
4
NAWA
11
10
9
7
CP
6
12
8
5
1
13
CHRISTIE
FOWLER
0 30 60 120 180 240
Kilometers

Figure 2.

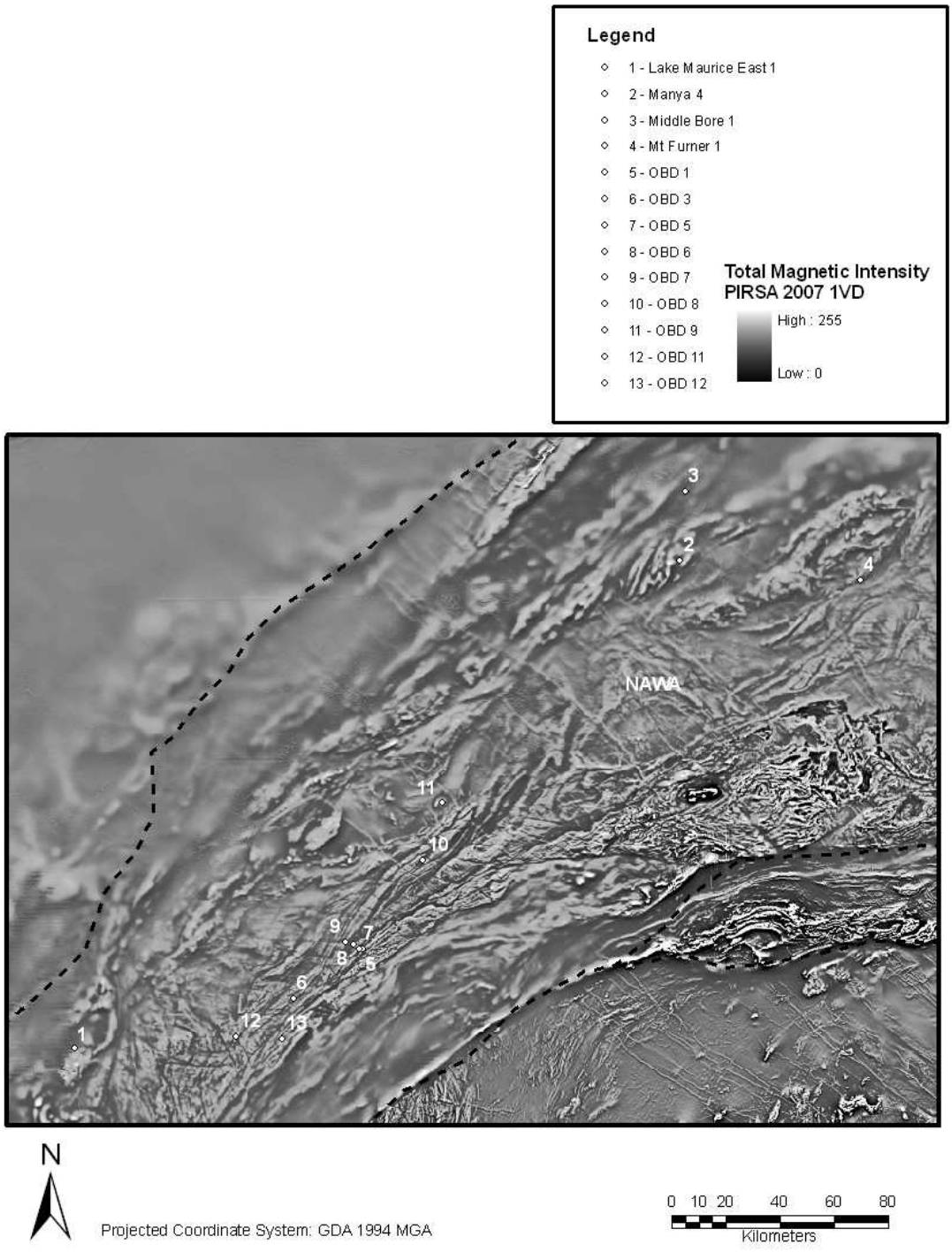
Legend
1 - Lake Maurice East 1
2 - Manya 4
3 - Middle Bore 1
4 - Mt Furner 1
5 - OBD 1
6 - OBD 3
7 - OBD 5
8 - OBD 6
9 - OBD 7
10 - OBD 8
11 - OBD 9
12 - OBD 11
13 - OBD 12
Total Magnetic Intensity
PIRSA 2007 1VD
High : 255
Low : 0
NAWA
N
Projected Coordinate System: GDA 1994 MGA
0 10 20 40 60 80
Kilometers

Figure 3.

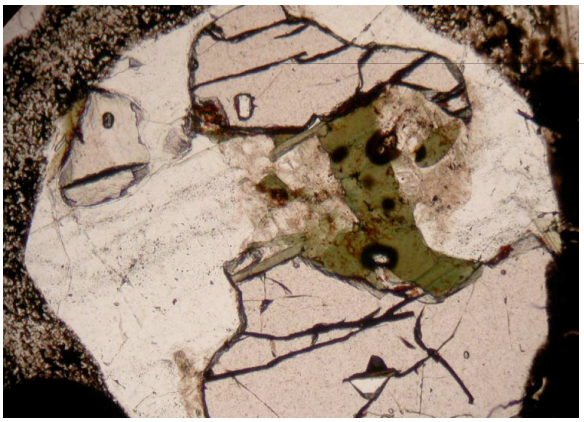

Manya 4
gt

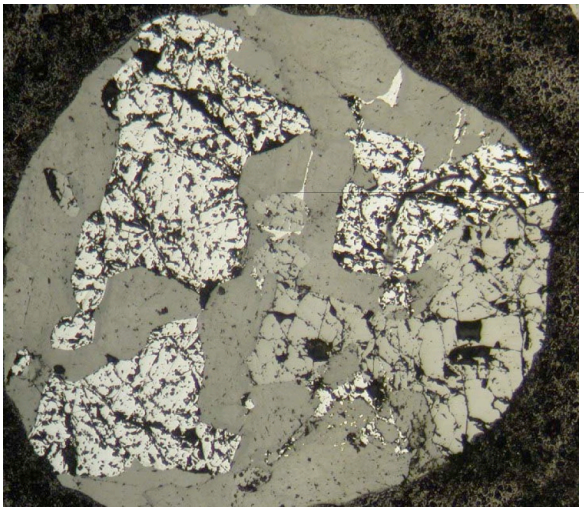

Middle Bore1
opaque

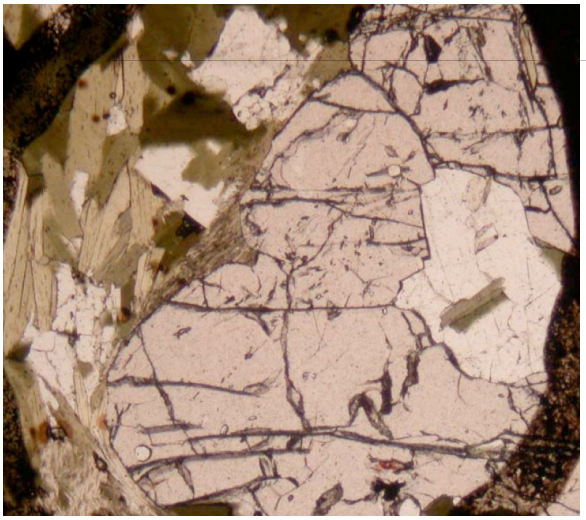

Mt Furner
Bi

Figure 4.

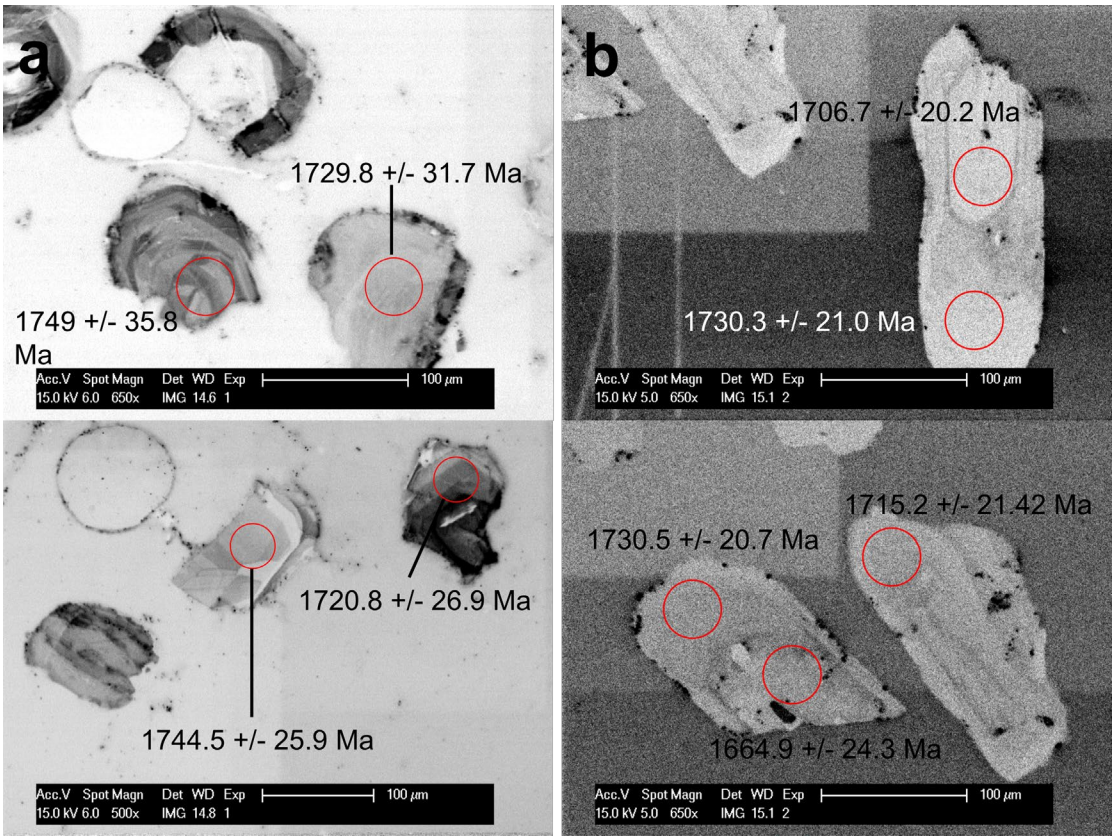
a
1729.8 +/- 31.7 Ma
1749 +/- 35.8 Ma
Acc.V Spot Magn Det WD Exp 100 µm
15.0 kV 6.0 650x IMG 14.6 1
1720.8 +/- 26.9 Ma
1744.5 +/- 25.9 Ma
Acc.V Spot Magn Det WD Exp 100 µm
15.0 kV 6.0 500x IMG 14.8 1
b
1706.7 +/- 20.2 Ma
1730.3 +/- 21.0 Ma
Acc.V Spot Magn Det WD Exp 100 µm
15.0 kV 5.0 650x IMG 15.1 2
1715.2 +/- 21.42 Ma
1730.5 +/- 20.7 Ma
1664.9 +/- 24.3 Ma
Acc.V Spot Magn Det WD Exp 100 µm
15.0 kV 5.0 650x IMG 15.1 2

Figure 5.

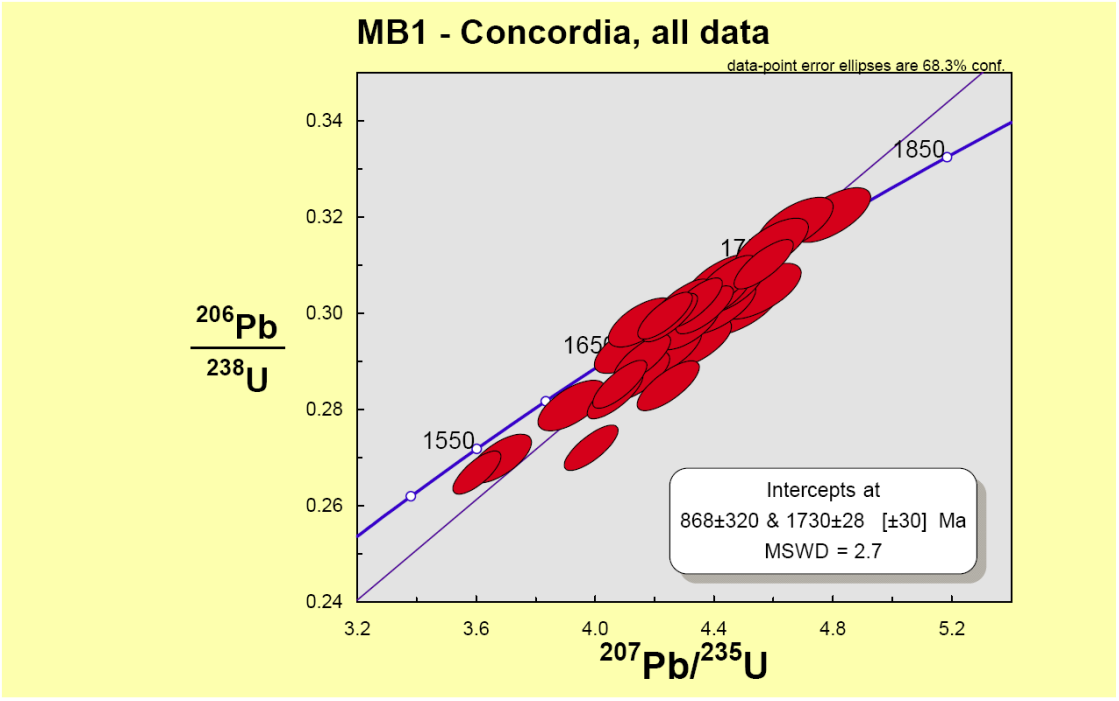
MB1 - Concordia, all data
data-point error ellipses are 68.3% conf.
206Pb/238U
207Pb/235U
0.34
0.32
0.30
0.28
0.26
0.24
3.2
3.6
4.0
4.4
4.8
5.2
1850
1550
Intercepts at
868±320 & 1730±28 [±30] Ma
MSWD = 2.7

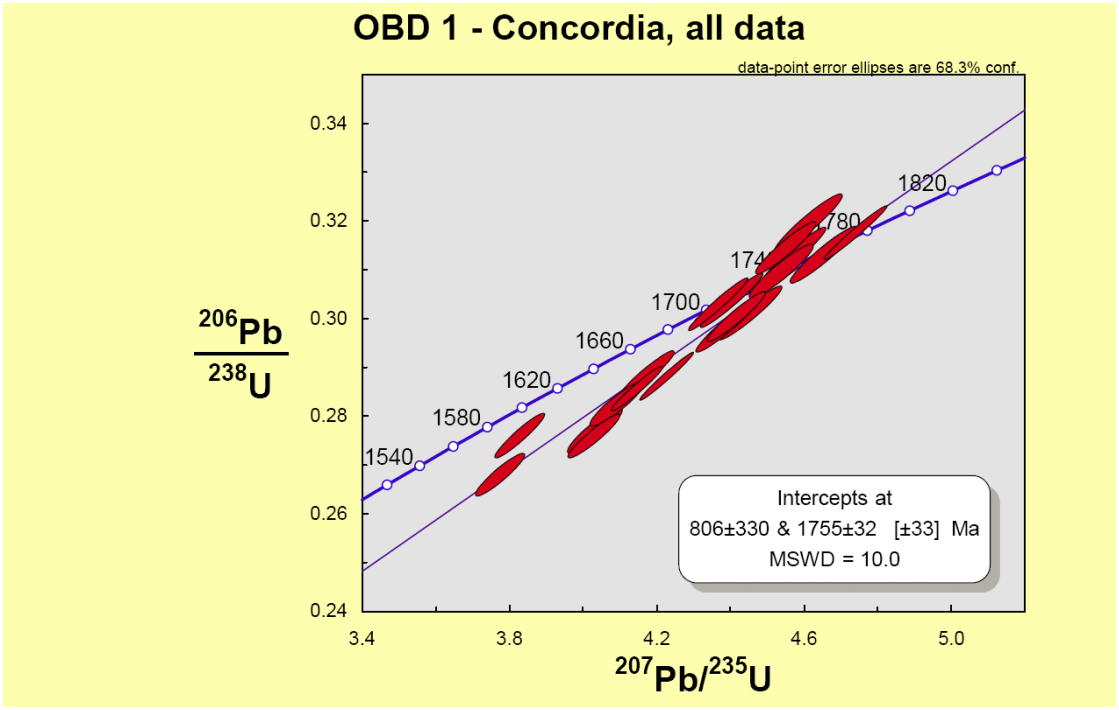
OBD 1 - Concordia, all data
data-point error ellipses are 68.3% conf.
206Pb/238U
207Pb/235U
0.34
0.32
0.30
0.28
0.26
0.24
3.4
3.8
4.2
4.6
5.0
1820
1700
1660
1620
1580
1540
Intercepts at
806±330 & 1755±32 [±33] Ma
MSWD = 10.0

Figure 5 (cont.)

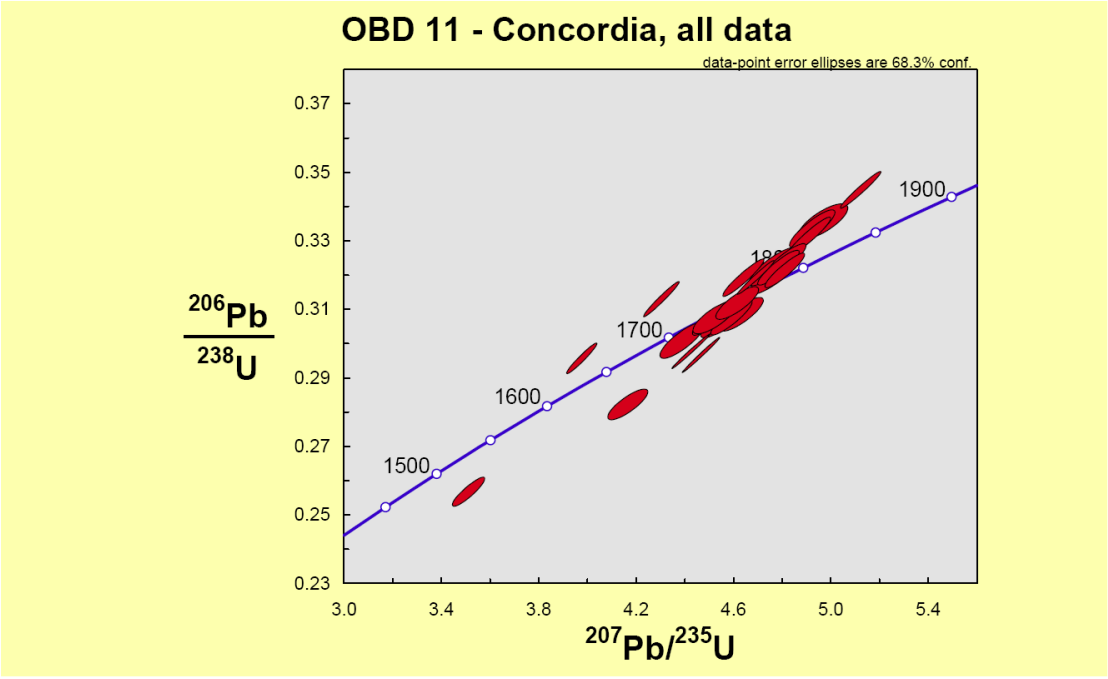

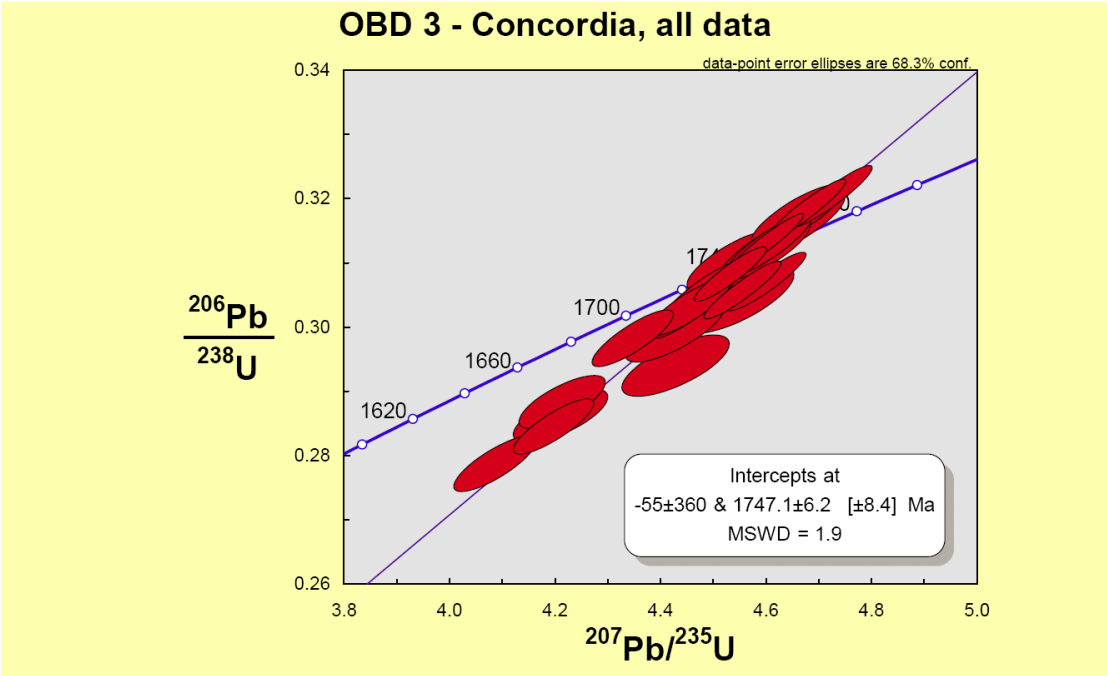

Figure 5 (cont.)

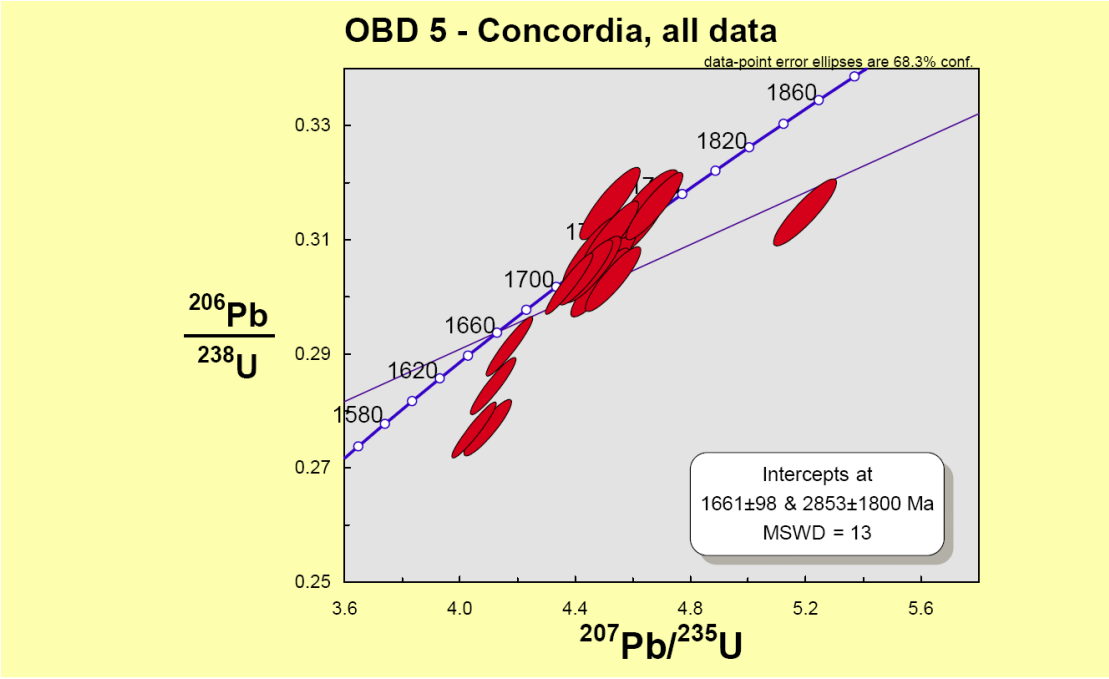

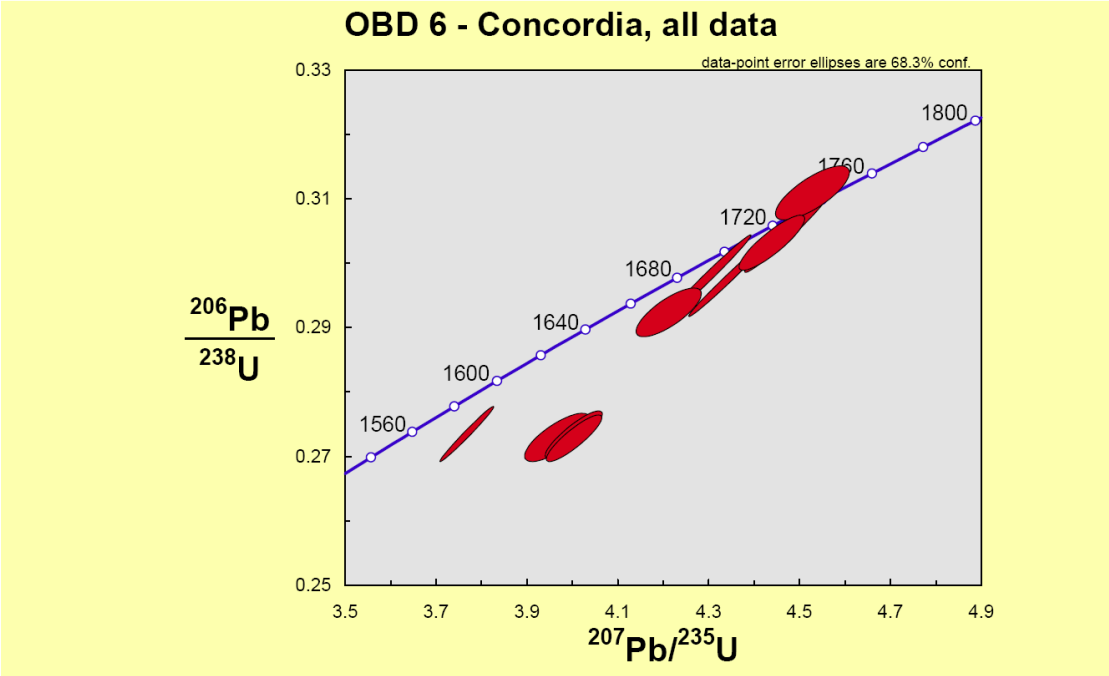

Figure 5 (cont.)

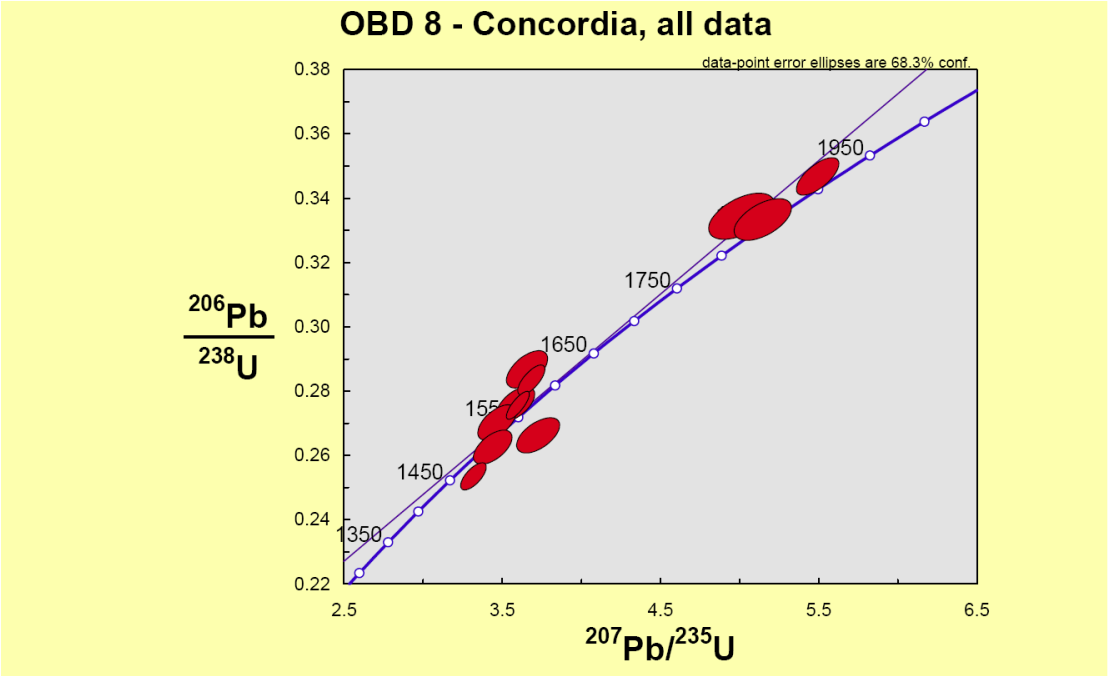

Figure 6.

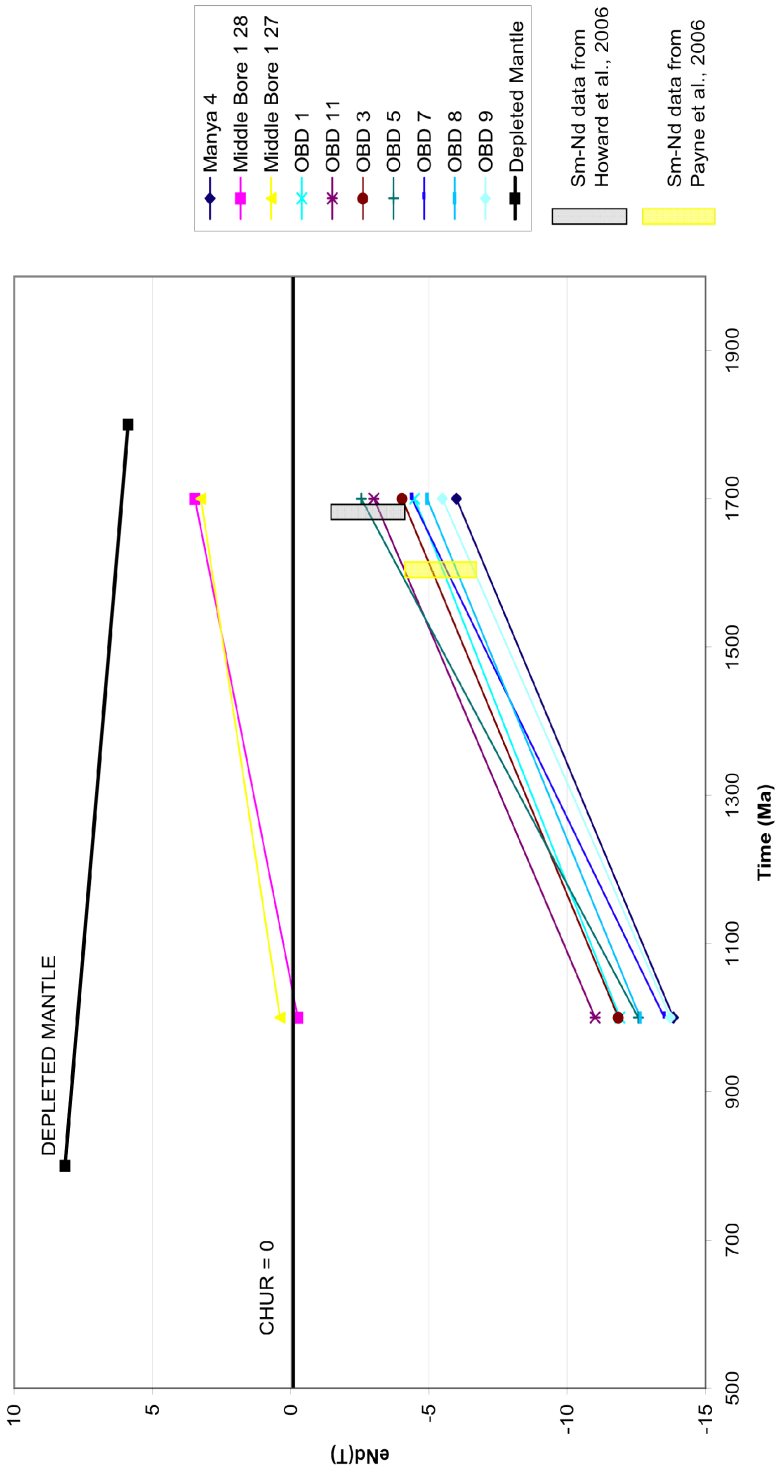
Manya 4
Middle Bore 1 28
Middle Bore 1 27
OBD 1
OBD 11
OBD 3
OBD 5
OBD 7
OBD 8
OBD 9
Depleted Mantle
Sm-Nd data from Howard et al., 2006
Sm-Nd data from Payne et al., 2006
DEPLETED MANTLE
CHUR = 0
εNd(T)
10
5
0
-5
-10
-15
500
700
900
1100
1300
1500
1700
1900
Time (Ma)

Figure 7.

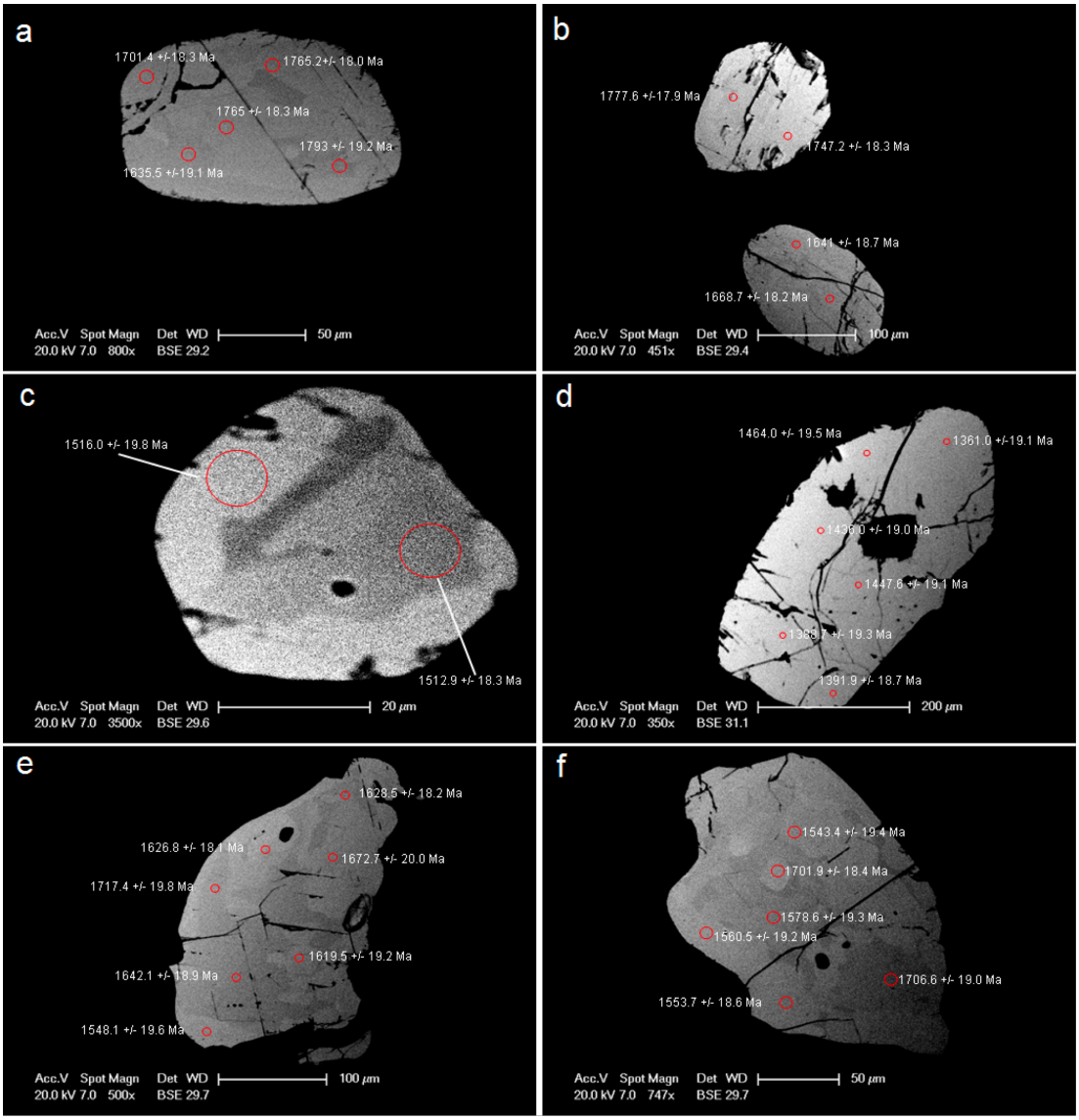
a
1701.4 +/-18.3 Ma
1765.2+/- 18.0 Ma
1765 +/- 18.3 Ma
1793 +/- 19.2 Ma
1635.5 +/-19.1 Ma
Acc.V Spot Magn Det WD 50 µm
20.0 kV 7.0 800x BSE 29.2
b
1777.6 +/-17.9 Ma
1747.2 +/- 18.3 Ma
1641 +/- 18.7 Ma
1668.7 +/- 18.2 Ma
Acc.V Spot Magn Det WD 100 µm
20.0 kV 7.0 451x BSE 29.4
c
1516.0 +/- 19.8 Ma
1512.9 +/- 18.3 Ma
Acc.V Spot Magn Det WD 20 µm
20.0 kV 7.0 3500x BSE 29.6
d
1464.0 +/- 19.5 Ma
1361.0 +/-19.1 Ma
1436.0 +/- 19.0 Ma
1447.6 +/- 19.1 Ma
1391.9 +/- 18.7 Ma
Acc.V Spot Magn Det WD 200 µm
20.0 kV 7.0 350x BSE 31.1
e
1628.5 +/- 18.2 Ma
1626.8 +/- 18.1 Ma
1672.7 +/- 20.0 Ma
1717.4 +/- 19.8 Ma
1619.5 +/- 19.2 Ma
1642.1 +/- 18.9 Ma
1548.1 +/- 19.6 Ma
Acc.V Spot Magn Det WD 100 µm
20.0 kV 7.0 500x BSE 29.7
f
1543.4 +/- 19.4 Ma
1701.9 +/- 18.4 Ma
1578.6 +/- 19.3 Ma
1560.5 +/- 19.2 Ma
1706.6 +/- 19.0 Ma
1553.7 +/- 18.6 Ma
Acc.V Spot Magn Det WD 50 µm
20.0 kV 7.0 747x BSE 29.7

Figure 8.

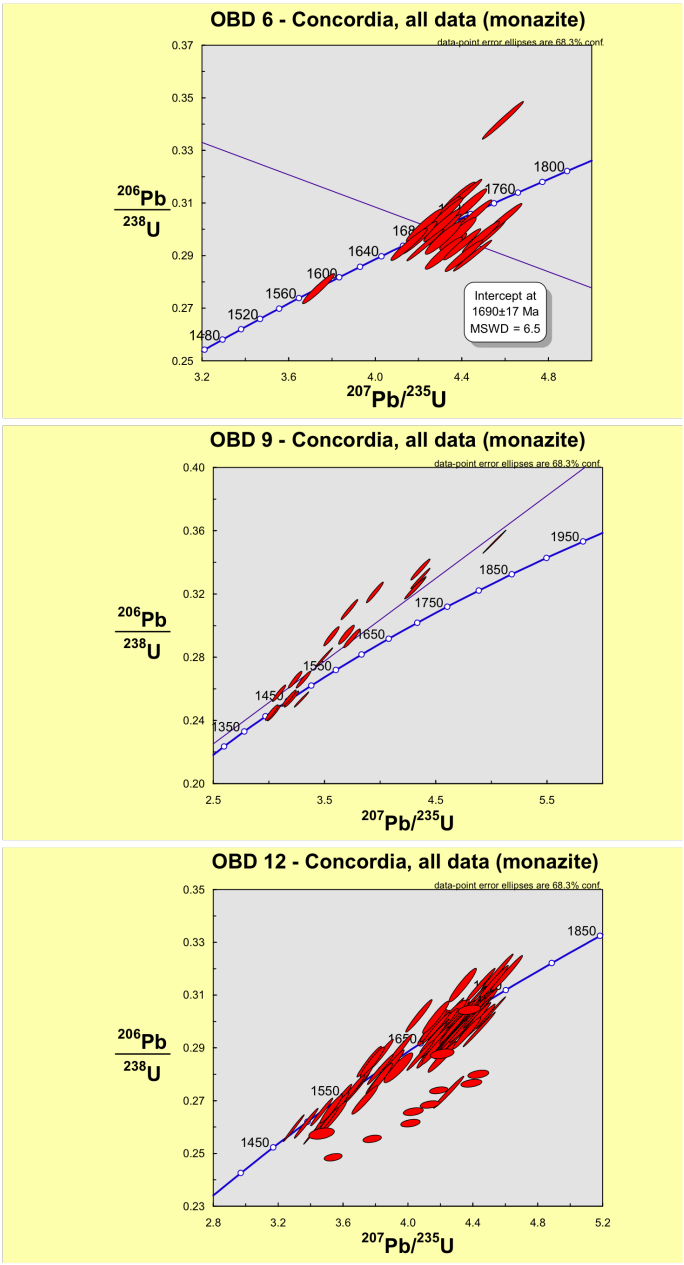
OBD 6 - Concordia, all data (monazite)
data-point error ellipses are 68.3% conf
Intercept at
1690±17 Ma
MSWD = 6.5
206Pb/238U
207Pb/235U
OBD 9 - Concordia, all data (monazite)
data-point error ellipses are 68.3% conf
206Pb/238U
207Pb/235U
OBD 12 - Concordia, all data (monazite)
data-point error ellipses are 68.3% conf
206Pb/238U
207Pb/235U

Figure 9.

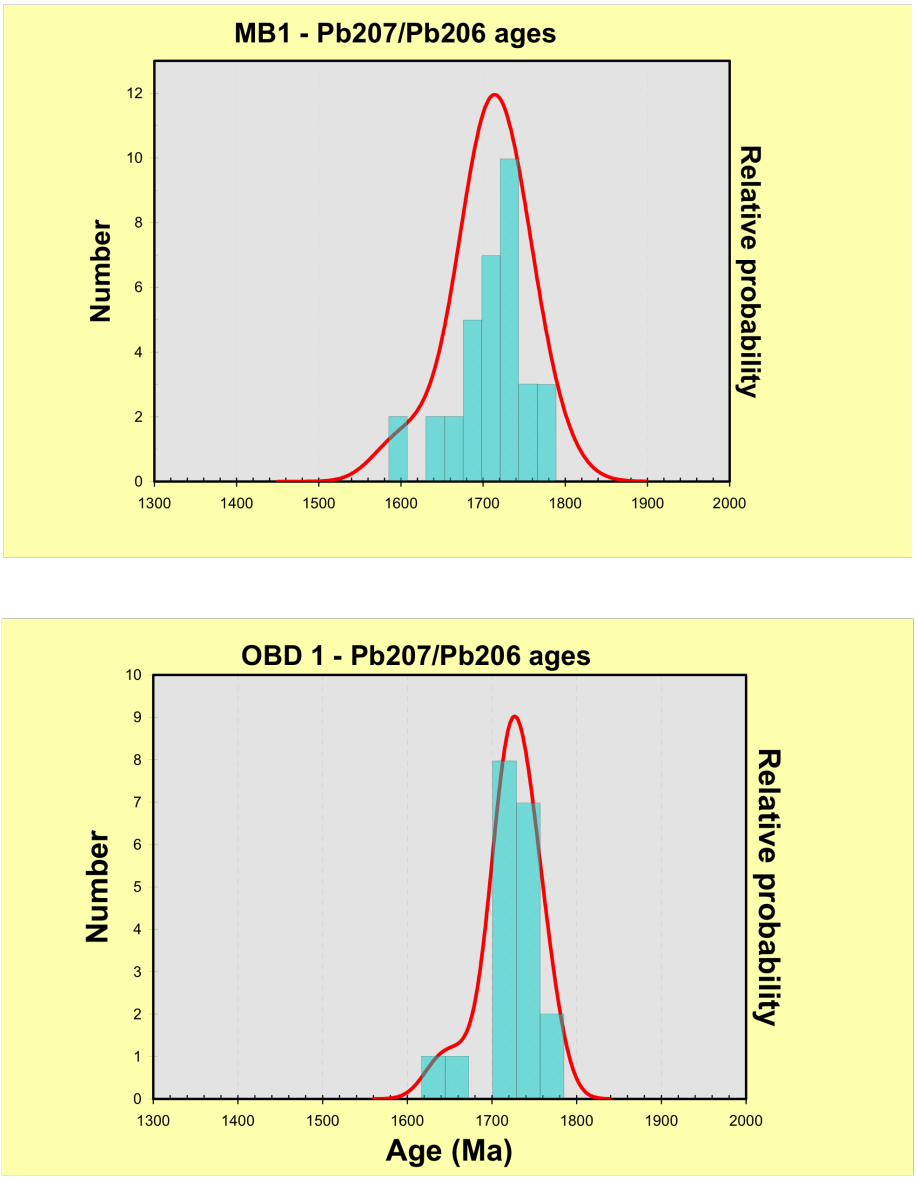
MB1 - Pb207/Pb206 ages
Number
Relative probability
0
2
4
6
8
10
12
1300
1400
1500
1600
1700
1800
1900
2000
OBD 1 - Pb207/Pb206 ages
Number
Relative probability
0
1
2
3
4
5
6
7
8
9
10
1300
1400
1500
1600
1700
1800
1900
2000
Age (Ma)

Figure 9 (cont).

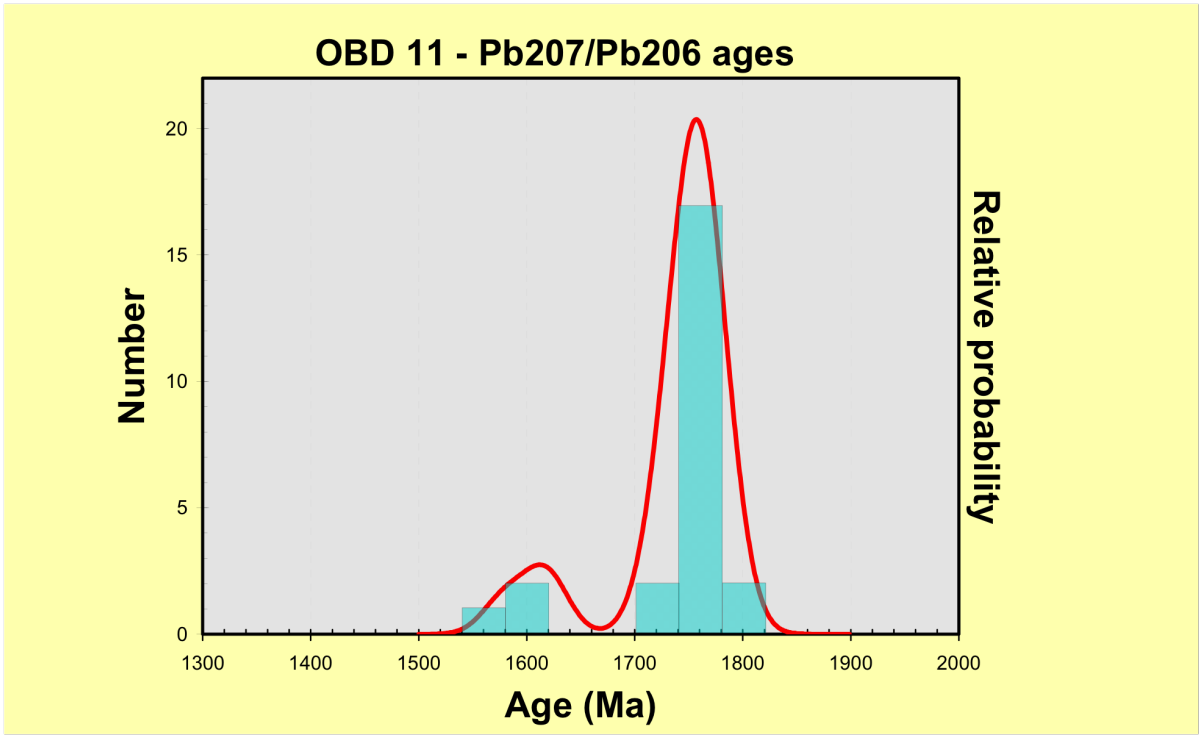

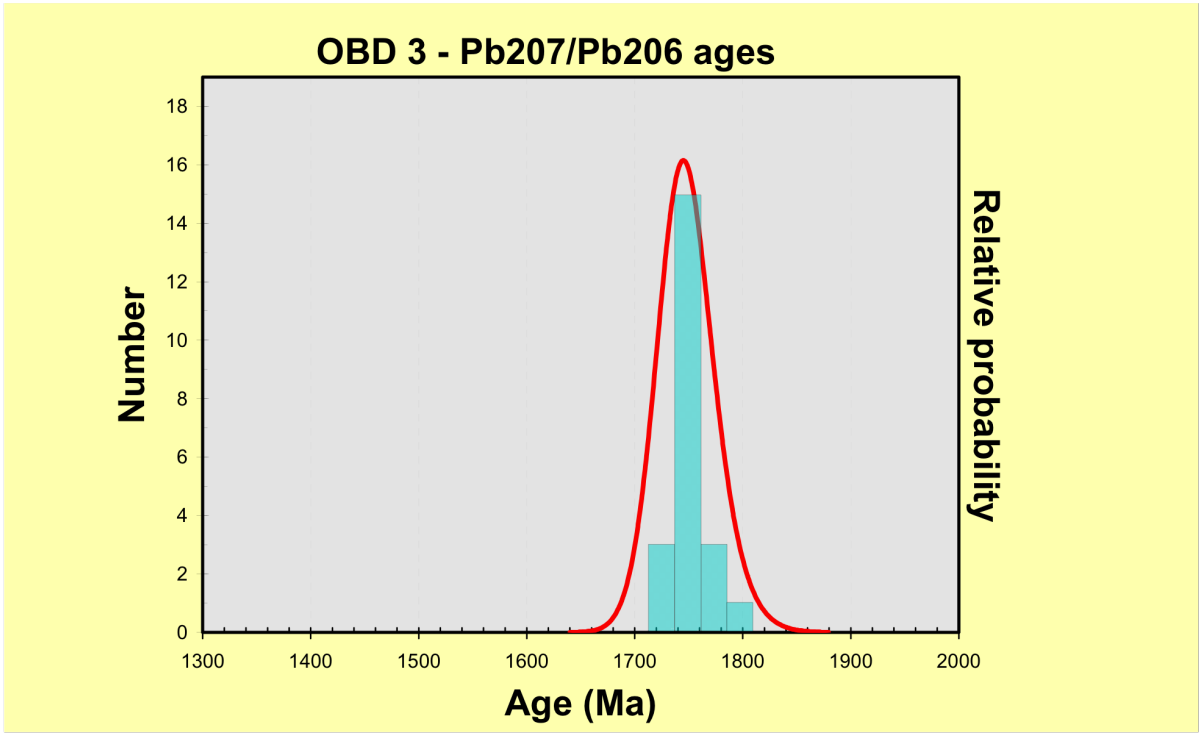

Figure 9 (cont).

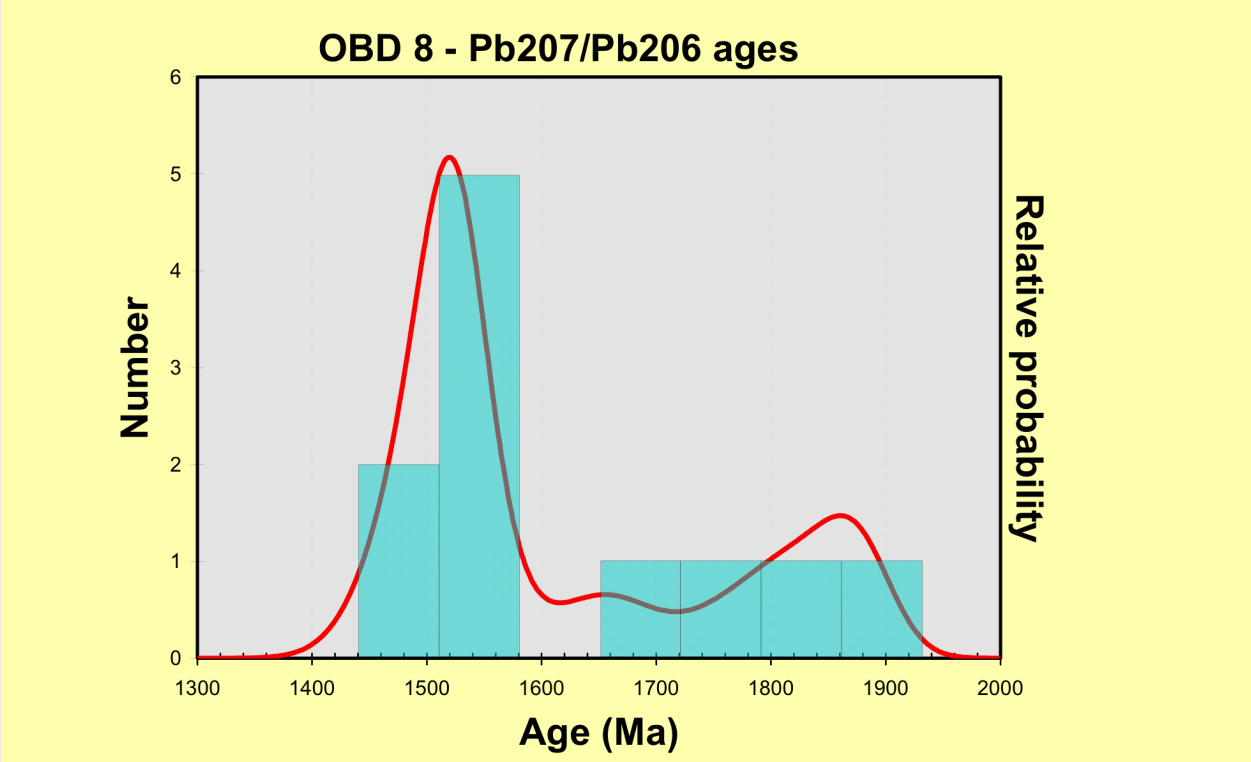

Figure 10.

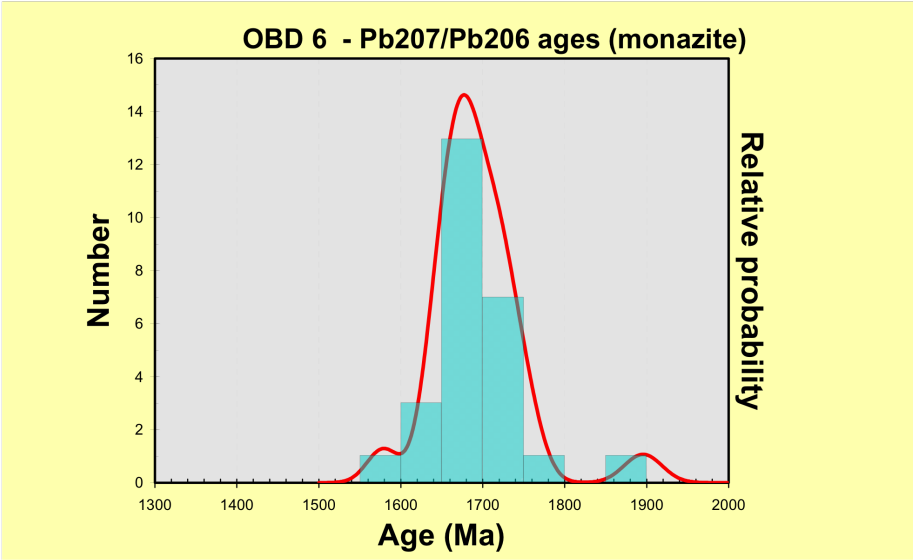
OBD 6 - Pb207/Pb206 ages (monazite)
Number
Relative probability
Age (Ma)
0
2
4
6
8
10
12
14
16
1300
1400
1500
1600
1700
1800
1900
2000

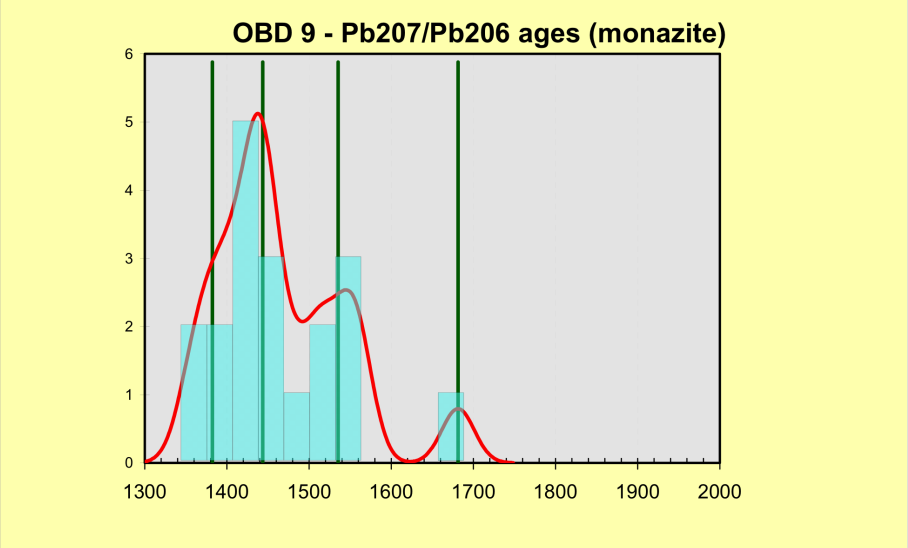
OBD 9 - Pb207/Pb206 ages (monazite)
0
1
2
3
4
5
6
1300
1400
1500
1600
1700
1800
1900
2000

Figure 10 (cont).

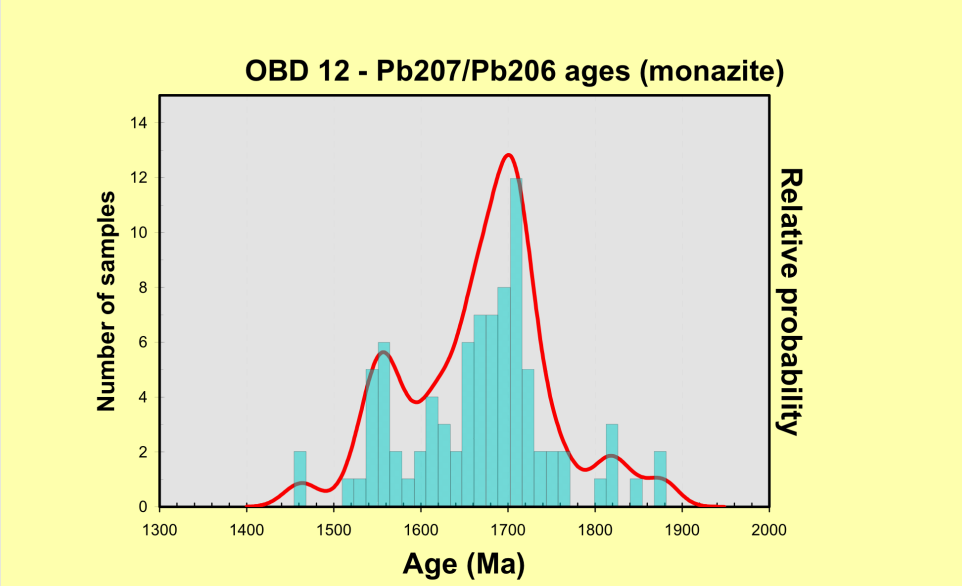

Figure 11

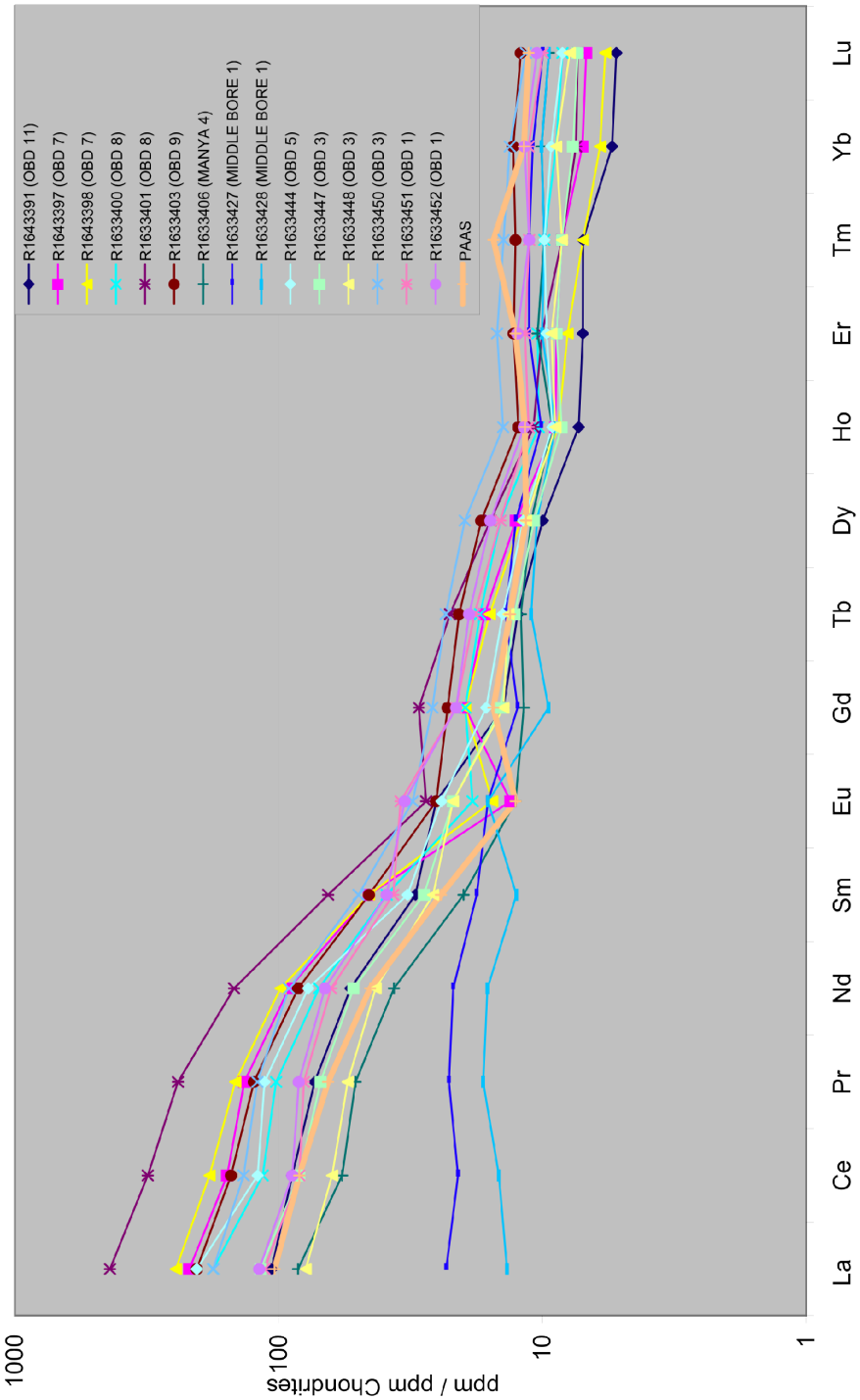
R1643391 (OBD 11)
R1643397 (OBD 7)
R1643398 (OBD 7)
R1633400 (OBD 8)
R1633401 (OBD 8)
R1633403 (OBD 9)
R1633406 (MANYA 4)
R1633427 (MIDDLE BORE 1)
R1633428 (MIDDLE BORE 1)
R1633444 (OBD 5)
R1633447 (OBD 3)
R1633448 (OBD 3)
R1633450 (OBD 3)
R1633451 (OBD 1)
R1633452 (OBD 1)
PAAS
La
Ce
Pr
Nd
Sm
Eu
Gd
Tb
Dy
Ho
Er
Tm
Yb
Lu
1000
100
10
1
ppm / ppm Chondrites

Figure 12.

Sample	Mineral assemblage	Temperature (°C)	±	Pressure (Kbar)	±	Age (Ma)	±
OBD 1	gt-cpx-opx-hbd-plag-ilm-qtz	779	59	7.9	1.2	1728	12
Middle Bore 1	gt-cpx-hbd-plag-mt-qtz	800	67	7.7	1.6	1713	11
Mt Furner	gt-bi-sill-plag-K-spar-sill-mu-qtz	709	58	5.8	1.6	1727.3	6
Manya 4	gt-bi-plag-ilm -qtz	750*		6.9	1.2	1719.3	7.9
OBD 3	gt-hbd-plag-qtz-mt	750*		9.1	1.9	1747.7	9.4
OBD 6	gt-bi-plag-ilm-qtz	800*		6.1	2.1	1731	14
OBD 7	gt-bi-plag-K-spar-mt-qtz	560	53	8	1	1751	9
OBD 9	gt-bi-plag-qtz	800*		4.8	2.1	1451	19
OBD 9	gt-bi-plag-qtz	800*		6.1	2.1	1451	19
OBD 12	gt-bi-plag-qtz	no result		no result			

- **Garnet-biotite Fe-Mg thermometry was used when insufficient mineral endmembers were available.**
- **Ages marked in blue are unpublished LA-ICP-MS zircon age results obtained by J.Payne**

Table 1.

Spot	Pb207/Pb206	1σ	207Pb/235U	ratios 1σ	Pb206/U238	1 sigma	Pb208/Th232	1σ
MB1-1	0.10809	0.00172	4.24698	0.06801	0.28499	0.00343	0.08626	0.0027
MB1-2	0.10384	0.00151	4.08485	0.06033	0.28532	0.0033	0.07749	0.00231
MB1-3	0.10432	0.00154	4.07205	0.06113	0.28313	0.0033	0.07854	0.00235
MB1-4	0.10637	0.00158	3.98973	0.05973	0.27205	0.00313	0.07491	0.00237
MB1-5	0.10405	0.00149	4.33718	0.06195	0.30234	0.00338	0.08335	0.0024
MB1-6	0.10674	0.00152	4.5685	0.06501	0.31044	0.00345	0.08593	0.00288
MB1-7	0.10537	0.00156	4.37071	0.0634	0.30085	0.00332	0.0813	0.00249
MB1-8	0.10778	0.00247	4.47513	0.0968	0.30123	0.00393	0.10031	0.00509
MB1-9	0.10381	0.00161	4.15965	0.06365	0.29064	0.00334	0.07772	0.00219
MB1-10	0.09804	0.00149	3.6066	0.05321	0.26682	0.00294	0.0696	0.00184
MB1-11	0.09906	0.00191	3.68422	0.06913	0.26978	0.00337	0.07276	0.00295
MB1-12	0.10844	0.00222	4.55674	0.08995	0.3048	0.0039	0.07879	0.00414
MB1-13	0.10534	0.00167	4.31885	0.06534	0.29739	0.00319	0.08093	0.00287
MB1-14	0.10856	0.00206	4.79896	0.08642	0.32065	0.00377	0.08612	0.00365
MB1-15	0.10114	0.00188	4.15722	0.0734	0.29815	0.00339	0.08036	0.00328
MB1-16	0.10308	0.00232	4.24058	0.09149	0.29837	0.00387	0.08045	0.00438
MB1-17	0.10194	0.00197	4.11691	0.07667	0.29293	0.00353	0.07795	0.00323
MB1-18	0.10308	0.00163	4.29331	0.06587	0.30209	0.00342	0.08442	0.00242
MB1-19	0.10556	0.00183	4.25153	0.07104	0.29213	0.00344	0.08493	0.0029
MB1-20	0.1048	0.00185	4.1463	0.07071	0.28698	0.00342	0.07598	0.00276
MB1-21	0.10263	0.00149	4.23821	0.05993	0.29955	0.00326	0.08312	0.00221
MB1-22	0.10638	0.002	4.41977	0.08073	0.30136	0.00371	0.08224	0.00316
MB1-23	0.1047	0.00189	4.35619	0.07624	0.3018	0.00363	0.0866	0.00349
MB1-24	0.10132	0.00203	3.92298	0.07578	0.28082	0.00349	0.08435	0.00439
MB1-25	0.10584	0.00218	4.35033	0.08638	0.29817	0.0038	0.08364	0.00386
MB1-26	0.10474	0.0018	4.34892	0.07249	0.30119	0.0035	0.08845	0.00373
MB1-27	0.10479	0.00213	4.4328	0.08621	0.30684	0.00379	0.09375	0.00429
MB1-28	0.10311	0.00147	4.25315	0.0602	0.29917	0.00332	0.08026	0.0023
MB1-29	0.10497	0.00166	4.44121	0.06837	0.30687	0.00349	0.08318	0.00259
MB1-30	0.10637	0.00204	4.67374	0.08491	0.31864	0.00376	0.08423	0.00392
MB1-31	0.10601	0.00198	4.59499	0.08194	0.31433	0.00373	0.08688	0.00359
MB1-32	0.107	0.00212	4.33456	0.08284	0.29381	0.00364	0.08659	0.00404
MB1-33	0.10589	0.00185	4.45772	0.07529	0.30536	0.00354	0.08556	0.00326
MB1-34	0.10533	0.0018	4.41431	0.0731	0.30396	0.00348	0.08317	0.00321
OBD1-1	0.11168	0.00129	5.69734	0.07136	0.36823	0.00422	0.10691	0.00238
OBD1-2	0.10642	0.00113	4.22915	0.04866	0.28822	0.00326	0.07674	0.00094
OBD1-3	0.10494	0.00119	4.17465	0.04991	0.2885	0.00326	0.07433	0.00089
OBD1-4	0.1049	0.0012	4.55121	0.05418	0.31465	0.00353	0.08016	0.00102
OBD1-5	0.10068	0.00113	3.83124	0.04455	0.27594	0.00304	0.07497	0.00097
OBD1-6	0.10559	0.00128	4.03406	0.04965	0.277	0.00309	0.07486	0.00097
OBD1-7	0.10529	0.00113	4.14898	0.04605	0.2857	0.00307	0.07931	0.00089
OBD1-8	0.10222	0.00118	3.77716	0.04422	0.26788	0.00291	0.07367	0.00092
OBD1-9	0.10593	0.0012	4.03153	0.04641	0.2759	0.00297	0.07971	0.00103
OBD1-10	0.10505	0.00123	4.09425	0.04827	0.28253	0.00305	0.08066	0.00117
OBD1-11	0.10457	0.00116	4.36814	0.05349	0.30302	0.00361	0.08316	0.00103
OBD1-12	0.10592	0.00122	4.57403	0.05766	0.31326	0.00378	0.08658	0.00112
OBD1-13	0.10627	0.00128	4.53906	0.05799	0.30986	0.0037	0.0868	0.00116
OBD1-14	0.10727	0.00125	4.4554	0.05666	0.30129	0.00365	0.08394	0.00107
OBD1-15	0.10513	0.00119	4.40436	0.05565	0.30389	0.00371	0.08304	0.00105
OBD1-16	0.10669	0.00123	4.38988	0.05472	0.29849	0.00354	0.082	0.00102
OBD1-17	0.10667	0.00122	4.41823	0.05233	0.30046	0.00338	0.08754	0.00113
OBD1-18	0.10775	0.00127	4.65381	0.06024	0.31328	0.00385	0.08564	0.00113
OBD1-19	0.10463	0.00125	4.61315	0.0605	0.3198	0.00396	0.08508	0.00115
OBD1-20	0.10819	0.00116	4.73988	0.05618	0.31779	0.0037	0.08367	0.00099

Spot	Apparent ages								%
	Pb207/Pb206	1σ	Pb207/U235	1σ	Pb206/U238	1σ	Pb208/Th232	1σ	Concordancy
MB1-1	1767.3	28.91	1616.5	17.18	1683.2	13.16	1672.3	50.22	91
MB1-2	1693.8	26.61	1618.1	16.53	1651.3	12.05	1508.4	43.28	96
MB1-3	1702.3	26.93	1607.1	16.6	1648.7	12.24	1528.3	44.09	94
MB1-4	1738	26.91	1551.2	15.86	1632.1	12.16	1460.1	44.63	89
MB1-5	1697.5	26.13	1702.9	16.74	1700.5	11.79	1618.1	44.85	100
MB1-6	1744.5	25.87	1742.9	16.99	1743.5	11.85	1666.3	53.54	100
MB1-7	1720.8	26.91	1695.5	16.45	1706.8	11.99	1580	46.6	99
MB1-8	1762.1	41.35	1697.4	19.46	1726.4	17.95	1932.2	93.44	96
MB1-9	1693.4	28.39	1644.7	16.7	1666.1	12.52	1512.8	41.07	97
MB1-10	1587.2	28.2	1524.7	14.97	1551	11.73	1360	34.78	96
MB1-11	1606.4	35.48	1539.7	17.1	1568	14.98	1419.6	55.59	96
MB1-12	1773.3	37.03	1715.1	19.28	1741.4	16.44	1533	77.54	97
MB1-13	1720.3	28.85	1678.3	15.85	1697	12.47	1573	53.7	98
MB1-14	1775.3	34.27	1792.9	18.38	1784.7	15.13	1669.7	67.87	101
MB1-15	1645.1	34.07	1682.2	16.82	1665.6	14.45	1562.2	61.36	102
MB1-16	1680.4	41.04	1683.2	19.24	1681.9	17.73	1564	82.03	100
MB1-17	1659.7	35.41	1656.2	17.62	1657.7	15.21	1517.1	60.54	100
MB1-18	1680.4	28.93	1701.7	16.94	1692.1	12.64	1638.1	45.12	101
MB1-19	1724.1	31.51	1652.2	17.14	1684	13.74	1647.5	53.99	96
MB1-20	1710.8	32.08	1626.4	17.14	1663.5	13.95	1480.1	51.79	95
MB1-21	1672.2	26.62	1689.1	16.19	1681.5	11.62	1613.8	41.25	101
MB1-22	1738.3	33.94	1698	18.37	1716.1	15.13	1597.5	59.09	98
MB1-23	1709	32.89	1700.2	17.95	1704.1	14.45	1678.8	65.01	99
MB1-24	1648.5	36.74	1595.5	17.58	1618.4	15.63	1636.8	81.83	97
MB1-25	1728.9	37.21	1682.2	18.87	1703	16.39	1623.6	71.98	97
MB1-26	1709.7	31.32	1697.2	17.34	1702.7	13.76	1713	69.32	99
MB1-27	1710.6	36.87	1725.2	18.68	1718.5	16.11	1811.3	79.28	101
MB1-28	1680.9	26.16	1687.2	16.5	1684.3	11.64	1560.4	42.95	100
MB1-29	1713.8	28.75	1725.3	17.21	1720.1	12.76	1615	48.31	101
MB1-30	1738	34.69	1783.1	18.4	1762.6	15.2	1634.6	73.1	103
MB1-31	1732	33.72	1762	18.28	1748.4	14.87	1684	66.72	102
MB1-32	1749	35.84	1660.5	18.14	1700	15.77	1678.5	75.22	95
MB1-33	1729.8	31.66	1717.8	17.47	1723.1	14.01	1659.3	60.74	99
MB1-34	1720.2	31.06	1710.9	17.18	1715	13.71	1614.8	59.94	99
OBD1-1	1827	20.85	1931	10.82	2021.1	19.89	2053	43.5	111
OBD1-2	1739	19.31	1679.7	9.45	1632.6	16.33	1494.4	17.64	94
OBD1-3	1713.3	20.68	1669.1	9.79	1634.1	16.33	1449.1	16.7	95
OBD1-4	1712.5	20.82	1740.4	9.91	1763.5	17.29	1558.5	19.11	103
OBD1-5	1636.7	20.65	1599.3	9.36	1570.9	15.35	1461.1	18.21	96
OBD1-6	1724.7	22.07	1641.1	10.02	1576.3	15.58	1459.1	18.28	91
OBD1-7	1719.4	19.67	1664	9.08	1620	15.41	1542.6	16.66	94
OBD1-8	1664.9	21.23	1587.9	9.4	1530	14.78	1436.7	17.3	92
OBD1-9	1730.5	20.73	1640.6	9.37	1570.7	14.99	1550.2	19.24	91
OBD1-10	1715.2	21.42	1653.2	9.62	1604.1	15.34	1567.9	21.86	94
OBD1-11	1706.7	20.23	1706.3	10.12	1706.3	17.85	1614.6	19.24	100
OBD1-12	1730.3	20.99	1744.5	10.5	1756.7	18.54	1678.3	20.81	102
OBD1-13	1736.3	21.89	1738.2	10.63	1740	18.23	1682.4	21.58	100
OBD1-14	1753.5	21.07	1722.7	10.55	1697.7	18.09	1629.1	19.93	97
OBD1-15	1716.6	20.71	1713.2	10.46	1710.5	18.35	1612.4	19.57	100
OBD1-16	1743.6	20.99	1710.4	10.31	1683.8	17.6	1593	19.06	97
OBD1-17	1743.3	20.74	1715.8	9.81	1693.6	16.73	1696.1	20.97	97
OBD1-18	1761.8	21.41	1759	10.82	1756.8	18.87	1660.7	21.11	100
OBD1-19	1707.9	21.8	1751.6	10.94	1788.8	19.36	1650.5	21.46	105
OBD1-20	1769	19.44	1774.3	9.94	1778.9	18.09	1624.1	18.55	101

Spot	Pb207/Pb206	1σ	207Pb/235U	ratios 1σ	Pb206/U238	1 sigma	Pb208/Th232	1σ
OBD1-21	0.11091	0.00142	4.593	0.06158	0.30043	0.00356	0.09519	0.00149
OBD1-22	0.10529	0.00119	4.38403	0.05357	0.30206	0.00348	0.08651	0.00114
OBD1-23	0.10688	0.00143	4.18229	0.05826	0.28384	0.00342	0.08131	0.00131
OBD1-24	0.1043	0.00125	4.06495	0.05198	0.28269	0.00331	0.08019	0.00117
OBD1-25	0.10636	0.00137	4.49288	0.06123	0.30638	0.00368	0.08922	0.00141
OBD1-26	0.10711	0.00122	4.52108	0.05619	0.30611	0.00358	0.09082	0.00121
OBD1-27	0.1063	0.00124	4.3129	0.05455	0.29422	0.00347	0.08478	0.00118
OBD1-28	0.10844	0.00117	4.5887	0.05508	0.30684	0.00358	0.08945	0.00111
OBD1-29	0.09862	0.00113	3.82411	0.04839	0.28132	0.00334	0.07846	0.00102
OBD1-30	0.10535	0.00122	4.33573	0.05566	0.29857	0.00358	0.08424	0.00113
OBD1-31	0.10783	0.00131	4.5562	0.06016	0.30651	0.00369	0.08395	0.00118
OBD1-32	0.10364	0.00127	4.06672	0.05509	0.28462	0.00352	0.08419	0.00126
OBD1-33	0.10572	0.00148	4.55767	0.06929	0.31267	0.00411	0.08868	0.0016
OBD3-1	-0.40973	0.98865	6.74677	52.23111	-0.46054	2.73589	-0.06405	0.09293
OBD3-2	0.10663	0.00118	4.53309	0.04507	0.30835	0.00282	0.08997	0.00113
OBD3-3	0.41364	1.51863	*********	*********	-23.31957	857.7675	-0.71739	2.07129
OBD3-4	0.10634	0.00124	4.48142	0.05096	0.30568	0.00313	0.09135	0.00134
OBD3-5	0.10642	0.00132	3.90725	0.04495	0.26631	0.00259	0.07692	0.0013
OBD3-6	0.11732	0.00155	3.98818	0.05085	0.24658	0.00263	0.0837	0.00116
OBD3-7	-0.31159	1.25914	-41.23595	160.93715	1.16489	2.71399	0.02726	0.27959
OBD3-8	7.50551	79.01237	*********	*********	-0.42362	4.73045	-0.66175	2.67595
OBD3-9	0.12281	0.00148	3.99662	0.0437	0.23605	0.00223	0.05804	0.00093
OBD3-10	0.10652	0.00114	4.60156	0.04592	0.31334	0.00296	0.09337	0.0011
OBD3-11	0.10708	0.00134	4.19928	0.05029	0.28446	0.00286	0.08867	0.00198
OBD3-12	0.10641	0.0014	4.08799	0.05184	0.27866	0.00287	0.08564	0.00211
OBD3-13	0.10659	0.00131	4.45509	0.05178	0.30316	0.00298	0.09078	0.002
OBD3-14	0.10688	0.00138	4.59887	0.05611	0.31208	0.0031	0.09146	0.00219
OBD3-15	0.10572	0.0013	4.34784	0.05065	0.29829	0.00292	0.08651	0.00197
OBD3-16	0.10726	0.00152	4.42835	0.06197	0.29946	0.00323	0.08758	0.00272
OBD3-17	0.10603	0.00148	4.21505	0.05397	0.28829	0.00274	0.08289	0.0025
OBD3-18	-0.54374	4.07647	-3.58795	13.69855	-0.49796	4.47716	-0.05003	0.21992
OBD3-19	0.10675	0.00161	4.2121	0.05889	0.2862	0.00279	0.08435	0.00299
OBD3-20	0.20441	1.02708	-0.84109	7.01272	-0.01808	0.07276	0.00247	0.01212
OBD3-21	0.10806	0.00119	4.55619	0.04807	0.30584	0.003	0.08854	0.00113
OBD3-22	0.10695	0.00118	4.72531	0.05032	0.32051	0.00318	0.08963	0.0012
OBD3-23	0.10676	0.00148	3.44853	0.04446	0.23435	0.00237	0.06841	0.00139
OBD3-24	0.39205	1.50968	2.30592	5.23921	-0.34554	1.05696	0.25316	1.1539
OBD3-25	0.11919	0.00143	4.72427	0.05496	0.28752	0.00297	0.10435	0.00171
OBD3-26	0.10866	0.00122	4.60112	0.04953	0.30717	0.00304	0.08895	0.00121
OBD3-27	0.11272	0.00119	4.39135	0.04418	0.28261	0.00273	0.09479	0.00117
OBD3-28	0.10677	0.00123	4.46188	0.05198	0.30314	0.00321	0.092	0.00141
OBD3-29	0.10655	0.00117	4.67751	0.04937	0.31846	0.00315	0.09298	0.00118
OBD3-30	0.20792	1.39267	24.49117	560.37592	20.91831	476.6616	-6.47999	149.59926
OBD3-31	0.10679	0.00128	4.60572	0.05395	0.31284	0.0032	0.09081	0.00191
OBD3-32	0.10929	0.00173	4.42968	0.06735	0.294	0.00318	0.08637	0.00302
OBD3-33	0.10698	0.00134	4.66269	0.05688	0.31613	0.00324	0.09275	0.0022
OBD3-34	0.10147	0.00152	3.30306	0.04701	0.23611	0.00246	0.07408	0.00243
OBD3-35	0.10841	0.00168	4.5484	0.06976	0.30436	0.00346	0.09727	0.00343
OBD3-36	0.10644	0.00137	4.65942	0.05709	0.31751	0.00319	0.09695	0.00242
OBD3-37	-0.00039	0.00975	-0.15243	3.89843	0.77401	4.01595	0.00652	0.02386
OBD3-38	0.1061	0.00146	4.541	0.05911	0.31043	0.00316	0.09194	0.00264

Spot	Pb207/Pb206	1σ	207Pb/235U	ratios 1σ	Pb206/U238	1 sigma	Pb208/Th232	1σ
MB1-1	0.10809	0.00172	4.24698	0.06801	0.28499	0.00343	0.08626	0.0027
MB1-2	0.10384	0.00151	4.08485	0.06033	0.28532	0.0033	0.07749	0.00231
MB1-3	0.10432	0.00154	4.07205	0.06113	0.28313	0.0033	0.07854	0.00235
MB1-4	0.10637	0.00158	3.98973	0.05973	0.27205	0.00313	0.07491	0.00237
MB1-5	0.10405	0.00149	4.33718	0.06195	0.30234	0.00338	0.08335	0.0024
MB1-6	0.10674	0.00152	4.5685	0.06501	0.31044	0.00345	0.08593	0.00288
MB1-7	0.10537	0.00156	4.37071	0.0634	0.30085	0.00332	0.0813	0.00249
MB1-8	0.10778	0.00247	4.47513	0.0968	0.30123	0.00393	0.10031	0.00509
MB1-9	0.10381	0.00161	4.15965	0.06365	0.29064	0.00334	0.07772	0.00219
MB1-10	0.09804	0.00149	3.6066	0.05321	0.26682	0.00294	0.0696	0.00184
MB1-11	0.09906	0.00191	3.68422	0.06913	0.26978	0.00337	0.07276	0.00295
MB1-12	0.10844	0.00222	4.55674	0.08995	0.3048	0.0039	0.07879	0.00414
MB1-13	0.10534	0.00167	4.31885	0.06534	0.29739	0.00319	0.08093	0.00287
MB1-14	0.10856	0.00206	4.79896	0.08642	0.32065	0.00377	0.08612	0.00365
MB1-15	0.10114	0.00188	4.15722	0.0734	0.29815	0.00339	0.08036	0.00328
MB1-16	0.10308	0.00232	4.24058	0.09149	0.29837	0.00387	0.08045	0.00438
MB1-17	0.10194	0.00197	4.11691	0.07667	0.29293	0.00353	0.07795	0.00323
MB1-18	0.10308	0.00163	4.29331	0.06587	0.30209	0.00342	0.08442	0.00242
MB1-19	0.10556	0.00183	4.25153	0.07104	0.29213	0.00344	0.08493	0.0029
MB1-20	0.1048	0.00185	4.1463	0.07071	0.28698	0.00342	0.07598	0.00276
MB1-21	0.10263	0.00149	4.23821	0.05993	0.29955	0.00326	0.08312	0.00221
MB1-22	0.10638	0.002	4.41977	0.08073	0.30136	0.00371	0.08224	0.00316
MB1-23	0.1047	0.00189	4.35619	0.07624	0.3018	0.00363	0.0866	0.00349
MB1-24	0.10132	0.00203	3.92298	0.07578	0.28082	0.00349	0.08435	0.00439
MB1-25	0.10584	0.00218	4.35033	0.08638	0.29817	0.0038	0.08364	0.00386
MB1-26	0.10474	0.0018	4.34892	0.07249	0.30119	0.0035	0.08845	0.00373
MB1-27	0.10479	0.00213	4.4328	0.08621	0.30684	0.00379	0.09375	0.00429
MB1-28	0.10311	0.00147	4.25315	0.0602	0.29917	0.00332	0.08026	0.0023
MB1-29	0.10497	0.00166	4.44121	0.06837	0.30687	0.00349	0.08318	0.00259
MB1-30	0.10637	0.00204	4.67374	0.08491	0.31864	0.00376	0.08423	0.00392
MB1-31	0.10601	0.00198	4.59499	0.08194	0.31433	0.00373	0.08688	0.00359
MB1-32	0.107	0.00212	4.33456	0.08284	0.29381	0.00364	0.08659	0.00404
MB1-33	0.10589	0.00185	4.45772	0.07529	0.30536	0.00354	0.08556	0.00326
MB1-34	0.10533	0.0018	4.41431	0.0731	0.30396	0.00348	0.08317	0.00321
OBD1-1	0.11168	0.00129	5.69734	0.07136	0.36823	0.00422	0.10691	0.00238
OBD1-2	0.10642	0.00113	4.22915	0.04866	0.28822	0.00326	0.07674	0.00094
OBD1-3	0.10494	0.00119	4.17465	0.04991	0.2885	0.00326	0.07433	0.00089
OBD1-4	0.1049	0.0012	4.55121	0.05418	0.31465	0.00353	0.08016	0.00102
OBD1-5	0.10068	0.00113	3.83124	0.04455	0.27594	0.00304	0.07497	0.00097
OBD1-6	0.10559	0.00128	4.03406	0.04965	0.277	0.00309	0.07486	0.00097
OBD1-7	0.10529	0.00113	4.14898	0.04605	0.2857	0.00307	0.07931	0.00089
OBD1-8	0.10222	0.00118	3.77716	0.04422	0.26788	0.00291	0.07367	0.00092
OBD1-9	0.10593	0.0012	4.03153	0.04641	0.2759	0.00297	0.07971	0.00103
OBD1-10	0.10505	0.00123	4.09425	0.04827	0.28253	0.00305	0.08066	0.00117
OBD1-11	0.10457	0.00116	4.36814	0.05349	0.30302	0.00361	0.08316	0.00103
OBD1-12	0.10592	0.00122	4.57403	0.05766	0.31326	0.00378	0.08658	0.00112
OBD1-13	0.10627	0.00128	4.53906	0.05799	0.30986	0.0037	0.0868	0.00116
OBD1-14	0.10727	0.00125	4.4554	0.05666	0.30129	0.00365	0.08394	0.00107
OBD1-15	0.10513	0.00119	4.40436	0.05565	0.30389	0.00371	0.08304	0.00105
OBD1-16	0.10669	0.00123	4.38988	0.05472	0.29849	0.00354	0.082	0.00102
OBD1-17	0.10667	0.00122	4.41823	0.05233	0.30046	0.00338	0.08754	0.00113
OBD1-18	0.10775	0.00127	4.65381	0.06024	0.31328	0.00385	0.08564	0.00113
OBD1-19	0.10463	0.00125	4.61315	0.0605	0.3198	0.00396	0.08508	0.00115
OBD1-20	0.10819	0.00116	4.73988	0.05618	0.31779	0.0037	0.08367	0.00099

Spot	Apparent ages								%
	Pb207/Pb206	1σ	Pb207/U235	1σ	Pb206/U238	1σ	Pb208/Th232	1σ	Concordancy
OBD5-1	1758.5	24.32	1728.8	12.42	1704.5	19.86	1513.2	22.79	97
OBD5-2	1714.7	24.92	1723.8	12.61	1731.5	20.33	1596.5	26.38	101
OBD5-3	1754.9	22.79	1763.2	11.51	1770.8	19.19	1690	24.6	101
OBD5-4	1716.3	20.7	1708.8	10.29	1703.3	17.63	1606.5	21.53	99
OBD5-5	1723.6	23.67	1735.3	12.01	1745.2	19.82	1578.7	25.31	101
OBD5-6	1874.2	19.66	1116.5	8.22	769.2	8.49	619.9	8.25	41
OBD5-7	1690	24.92	1735.2	12.6	1773	20.83	1694.8	29.28	105
OBD5-8	1695.5	21.08	1669.2	10.43	1648.5	17.43	1581.7	21.04	97
OBD5-9	1951.7	22.95	1852.4	11.81	1765.3	19.11	2067.6	31.11	90
OBD5-10	1749.7	23.34	1582.4	11.12	1460.4	16.03	1157.9	21.42	83
OBD5-11	1744.5	26.26	1732.8	13.04	1722.9	20.11	1562.3	24.76	99
OBD5-12	1728.4	22.86	1719.8	11.42	1713.1	18.65	1594.6	21.01	99
OBD5-13	1746.5	27.23	1749.9	13.31	1753	20.27	1634.8	27.94	100
OBD5-14	1742.3	26.35	1758.6	12.72	1772.6	19.67	1782.6	29.45	102
OBD5-15	1736.7	20.61	1644.9	10.14	1574.3	16.39	1237.7	14.46	91
OBD5-16	1753.5	23.45	1050.8	8.86	746.3	8.32	558.9	8	43
OBD5-17	1773.1	23.29	1737.2	11.71	1707.6	18.82	1374.5	19.85	96
OBD5-18	1715.7	20.94	1658.1	10.28	1613.5	16.77	1415.7	16.61	94
OBD5-19	1734.1	24.21	1724.1	11.99	1716	19.01	1535.7	23.82	99
OBD5-20	1755.6	22.16	1654.5	10.79	1576.4	16.78	1227.6	16.4	90
OBD6-1	1714.1	18.21	1582.9	8.7	1486.6	14.49	1367.4	11.4	87
OBD6-2	1762.1	21.85	1586.9	9.39	1458.9	13.49	1480.2	14.24	83
OBD6-3	1710.2	18.49	1694	11.41	1681.4	20.71	1476.4	14.21	98
OBD6-4	1730.2	18.93	1700.7	10.22	1677.1	18.08	1769.4	17.47	97
OBD6-5	1740.9	19.39	1725.7	11.09	1713.8	19.69	1821	19.68	98
OBD6-6	1625.9	19.14	1586.6	8.42	1558.1	14.32	1458.8	12.27	96
OBD6-7	2000	0	-NaN	-NaN	-NaN	NaN	-NaN	NaN	#VALUE!
OBD6-8	4368.7	3631.26	3694	*******	-NaN	*******	-152.9	268.38	#VALUE!
OBD6-9	1642	65.89	1347.7	27.3	1170.2	13.26	1206.9	16.17	71
OBD6-10	5691.6	1063.1	-NaN	-630.17	******	3689.98	******	6992.69	#VALUE!
OBD6-11	1648.1	22.2	1094.1	9.36	837.6	10.09	982.2	11.34	51
OBD6-12	2045.8	18.03	1033.4	7.29	623.5	6.61	1928.1	16.76	30
OBD6-13	19.51	7436	7.75	87475	13.15	1764	19.95	9439	67
OBD6-14	7791.03	6001	*******	46	*******	1310	*******	59	#VALUE!
OBD6-15	19.86	7110	7.6	126658	12.14	1691	21.79	13811	61
OBD6-16	21.43	6704	7.61	60121	10.82	1580	22.05	5867	50
OBD6-17	22.52	7101	9.09	337123	12.96	1655	38.96	36086	58
OBD6-18	7999.9	5401	4975.79	42	6670.85	1235	1621.28	28	83
OBD6-19	20.62	6798	8.38	91069	13.54	1562	27.61	9740	66
OBD6-20	427.99	5845	*******	29	3015.07	1205	*******	49	704
OBD6-21	22.03	7193	9.47	122282	14.56	1608	35.09	13115	66
OBD6-22	1871.2	20.93	1718.8	8.57	1596.7	12.75	1980.4	29.3	85
OBD6-23	24.09	6987	10.26	58870	14.23	1652	35.78	6315	59
OBD6-24	0.1	4412.72	-99.3	1024.38	1655.6	6162.38	******	*******	1655600
OBD6-25	1735.9	22.49	1448.8	8.05	1261.3	9.53	1492	29.18	73
OBD6-26	1735.9	21.46	1719.7	8.88	1706.7	13.99	1815.5	27.5	98
OBD6-27	1740.8	20.76	1635.3	8.14	1554.7	12.2	1016.3	15.59	89
OBD6-28	1737.3	21.06	1635.3	8.46	1557.3	12.58	1351.2	23.14	90
OBD6-29	1723.1	24.13	1627.8	9.6	1555.3	12.51	1720.9	41.5	90
OBD6-30	4413.4	2902.3	244.2	423.28	161.3	585.5	1783.2	*******	4
OBD6-31	1706.9	23.59	1676.7	9.16	1652.9	12.52	1697	37.64	97
OBD6-32	0.1	6125.46	612.2	1803.98	-531.9	1775.97	1304.8	4250.2	-531900
OBD6-33	1725.9	24.41	1736.1	9.84	1744.9	13.69	1783	40.99	101

Spot	Pb207/Pb206	1σ	207Pb/235U	ratios 1σ	Pb206/U238	1 sigma	Pb208/Th232	1σ
OBD8-1	0.09487	0.00126	3.60431	0.04773	0.27554	0.00291	0.08656	0.00287
OBD8-2	0.1148	0.00192	5.49501	0.08952	0.34717	0.00385	0.1115	0.00509
OBD8-3	0.10353	0.00165	3.72558	0.05903	0.26101	0.0029	0.09308	0.00413
OBD8-4	0.1011	0.00165	3.57214	0.05845	0.2563	0.00289	0.09731	0.00465
OBD8-5	0.09444	0.00142	3.6907	0.05662	0.28353	0.00311	0.08916	0.00404
OBD8-6	0.0952	0.00218	3.44643	0.08044	0.26253	0.00353	0.09346	0.00705
OBD8-7	0.10872	0.00287	5.01436	0.13524	0.33469	0.00478	0.10755	0.00967
OBD8-8	0.11214	0.00243	5.14936	0.1194	0.33363	0.00428	0.0974	0.00776
OBD8-9	0.09445	0.00197	3.58911	0.08031	0.27586	0.0036	0.08624	0.00622
OBD8-10	0.09269	0.00201	3.66155	0.08586	0.28677	0.00385	0.08606	0.00643
OBD8-11	0.09332	0.00199	3.47266	0.07952	0.27013	0.00365	0.09215	0.00688
OBD8-12	0.10116	0.00174	3.46443	0.05934	0.24838	0.0029	0.17643	0.00904
OBD8-13	0.09366	0.00171	2.86555	0.0514	0.22193	0.00258	0.0485	0.00266
OBD8-14	0.10165	0.00242	3.73122	0.08898	0.26617	0.00363	0.0764	0.00598
OBD8-15	0.09629	0.00174	2.89268	0.05145	0.21787	0.00252	0.0547	0.00292
OBD8-16	0.09509	0.00155	3.32196	0.05336	0.25338	0.0028	0.08739	0.00423
OBD8-17	0.05918	0.00121	0.82485	0.01645	0.1011	0.00118	0.03335	0.00218
OBD11-1	0.10649	0.00111	4.69209	0.04933	0.3195	0.00329	0.10187	0.001
OBD11-2	0.09976	0.00105	4.30595	0.04813	0.31311	0.00342	0.11098	0.00115
OBD11-3	0.11004	0.00118	3.32767	0.03776	0.21934	0.00241	0.10421	0.00109
OBD11-4	0.10746	0.00121	4.91271	0.05837	0.33158	0.00372	0.10594	0.00123
OBD11-5	0.09758	0.00103	3.97953	0.04115	0.2958	0.00295	0.08943	0.00097
OBD11-6	0.10543	0.00118	4.6428	0.05565	0.31946	0.00362	0.10746	0.00131
OBD11-7	0.10784	0.00111	4.42763	0.051	0.29787	0.00341	0.09783	0.00099
OBD11-8	0.10758	0.00113	5.12174	0.05452	0.34523	0.00358	0.1189	0.00117
OBD11-9	25.21856	*********	-4.58575	104.20189	-0.07631	4.99839	0.02858	0.01847
OBD11-10	0.10922	0.00112	4.46717	0.05066	0.29672	0.00334	0.09905	0.00099
OBD11-11	0.10853	0.00123	4.81139	0.05477	0.32159	0.00335	0.10045	0.00188
OBD11-12	0.10892	0.00141	4.63468	0.05956	0.30865	0.00329	0.10285	0.00281
OBD11-13	0.0994	0.00117	3.51581	0.04304	0.25658	0.00282	0.09799	0.00228
OBD11-14	0.10653	0.00128	4.51823	0.05622	0.30765	0.00338	0.09856	0.0023
OBD11-15	0.10701	0.00131	4.92415	0.06154	0.33378	0.00364	0.10638	0.0025
OBD11-16	0.10728	0.00153	4.96885	0.06734	0.33598	0.00344	0.10475	0.0035
OBD11-17	0.10581	0.0014	4.39063	0.06035	0.30099	0.00346	0.1047	0.00304
OBD11-18	0.10733	0.00139	4.61665	0.0578	0.31202	0.00319	0.10058	0.00288
OBD11-19	0.10826	0.00128	4.59262	0.05558	0.30774	0.00332	0.10212	0.00237
OBD11-20	0.10716	0.00139	4.16847	0.0535	0.28219	0.00299	0.09678	0.0027
OBD11-21	0.1077	0.00142	4.56112	0.06292	0.30722	0.00358	0.104	0.00277
OBD11-22	0.10769	0.00125	4.78646	0.05574	0.3224	0.00338	0.10227	0.00219
OBD11-23	0.10665	0.00145	4.5232	0.05889	0.30764	0.00313	0.11101	0.00346
OBD11-24	0.10708	0.00138	4.76276	0.06395	0.32266	0.00369	0.10477	0.00294
OBD11-25	0.10764	0.00129	4.80818	0.05875	0.32401	0.0035	0.10486	0.00249
OBD11-26	0.10799	0.00142	4.76643	0.06554	0.32016	0.00369	0.10155	0.003
OBD11-27	0.73798	9.82273	-8.04047	86.46568	-0.03421	0.24586	-0.78982	9.63861

Spot	Pb207/Pb206	1σ	207Pb/235U	ratios 1σ	Pb206/U238	1 sigma	Pb208/Th232	1σ
MB1-1	0.10809	0.00172	4.24698	0.06801	0.28499	0.00343	0.08626	0.0027
MB1-2	0.10384	0.00151	4.08485	0.06033	0.28532	0.0033	0.07749	0.00231
MB1-3	0.10432	0.00154	4.07205	0.06113	0.28313	0.0033	0.07854	0.00235
MB1-4	0.10637	0.00158	3.98973	0.05973	0.27205	0.00313	0.07491	0.00237
MB1-5	0.10405	0.00149	4.33718	0.06195	0.30234	0.00338	0.08335	0.0024
MB1-6	0.10674	0.00152	4.5685	0.06501	0.31044	0.00345	0.08593	0.00288
MB1-7	0.10537	0.00156	4.37071	0.0634	0.30085	0.00332	0.0813	0.00249
MB1-8	0.10778	0.00247	4.47513	0.0968	0.30123	0.00393	0.10031	0.00509
MB1-9	0.10381	0.00161	4.15965	0.06365	0.29064	0.00334	0.07772	0.00219
MB1-10	0.09804	0.00149	3.6066	0.05321	0.26682	0.00294	0.0696	0.00184
MB1-11	0.09906	0.00191	3.68422	0.06913	0.26978	0.00337	0.07276	0.00295
MB1-12	0.10844	0.00222	4.55674	0.08995	0.3048	0.0039	0.07879	0.00414
MB1-13	0.10534	0.00167	4.31885	0.06534	0.29739	0.00319	0.08093	0.00287
MB1-14	0.10856	0.00206	4.79896	0.08642	0.32065	0.00377	0.08612	0.00365
MB1-15	0.10114	0.00188	4.15722	0.0734	0.29815	0.00339	0.08036	0.00328
MB1-16	0.10308	0.00232	4.24058	0.09149	0.29837	0.00387	0.08045	0.00438
MB1-17	0.10194	0.00197	4.11691	0.07667	0.29293	0.00353	0.07795	0.00323
MB1-18	0.10308	0.00163	4.29331	0.06587	0.30209	0.00342	0.08442	0.00242
MB1-19	0.10556	0.00183	4.25153	0.07104	0.29213	0.00344	0.08493	0.0029
MB1-20	0.1048	0.00185	4.1463	0.07071	0.28698	0.00342	0.07598	0.00276
MB1-21	0.10263	0.00149	4.23821	0.05993	0.29955	0.00326	0.08312	0.00221
MB1-22	0.10638	0.002	4.41977	0.08073	0.30136	0.00371	0.08224	0.00316
MB1-23	0.1047	0.00189	4.35619	0.07624	0.3018	0.00363	0.0866	0.00349
MB1-24	0.10132	0.00203	3.92298	0.07578	0.28082	0.00349	0.08435	0.00439
MB1-25	0.10584	0.00218	4.35033	0.08638	0.29817	0.0038	0.08364	0.00386
MB1-26	0.10474	0.0018	4.34892	0.07249	0.30119	0.0035	0.08845	0.00373
MB1-27	0.10479	0.00213	4.4328	0.08621	0.30684	0.00379	0.09375	0.00429
MB1-28	0.10311	0.00147	4.25315	0.0602	0.29917	0.00332	0.08026	0.0023
MB1-29	0.10497	0.00166	4.44121	0.06837	0.30687	0.00349	0.08318	0.00259
MB1-30	0.10637	0.00204	4.67374	0.08491	0.31864	0.00376	0.08423	0.00392
MB1-31	0.10601	0.00198	4.59499	0.08194	0.31433	0.00373	0.08688	0.00359
MB1-32	0.107	0.00212	4.33456	0.08284	0.29381	0.00364	0.08659	0.00404
MB1-33	0.10589	0.00185	4.45772	0.07529	0.30536	0.00354	0.08556	0.00326
MB1-34	0.10533	0.0018	4.41431	0.0731	0.30396	0.00348	0.08317	0.00321
OBD1-1	0.11168	0.00129	5.69734	0.07136	0.36823	0.00422	0.10691	0.00238
OBD1-2	0.10642	0.00113	4.22915	0.04866	0.28822	0.00326	0.07674	0.00094
OBD1-3	0.10494	0.00119	4.17465	0.04991	0.2885	0.00326	0.07433	0.00089
OBD1-4	0.1049	0.0012	4.55121	0.05418	0.31465	0.00353	0.08016	0.00102
OBD1-5	0.10068	0.00113	3.83124	0.04455	0.27594	0.00304	0.07497	0.00097
OBD1-6	0.10559	0.00128	4.03406	0.04965	0.277	0.00309	0.07486	0.00097
OBD1-7	0.10529	0.00113	4.14898	0.04605	0.2857	0.00307	0.07931	0.00089
OBD1-8	0.10222	0.00118	3.77716	0.04422	0.26788	0.00291	0.07367	0.00092
OBD1-9	0.10593	0.0012	4.03153	0.04641	0.2759	0.00297	0.07971	0.00103
OBD1-10	0.10505	0.00123	4.09425	0.04827	0.28253	0.00305	0.08066	0.00117
OBD1-11	0.10457	0.00116	4.36814	0.05349	0.30302	0.00361	0.08316	0.00103
OBD1-12	0.10592	0.00122	4.57403	0.05766	0.31326	0.00378	0.08658	0.00112
OBD1-13	0.10627	0.00128	4.53906	0.05799	0.30986	0.0037	0.0868	0.00116
OBD1-14	0.10727	0.00125	4.4554	0.05666	0.30129	0.00365	0.08394	0.00107
OBD1-15	0.10513	0.00119	4.40436	0.05565	0.30389	0.00371	0.08304	0.00105
OBD1-16	0.10669	0.00123	4.38988	0.05472	0.29849	0.00354	0.082	0.00102
OBD1-17	0.10667	0.00122	4.41823	0.05233	0.30046	0.00338	0.08754	0.00113
OBD1-18	0.10775	0.00127	4.65381	0.06024	0.31328	0.00385	0.08564	0.00113
OBD1-19	0.10463	0.00125	4.61315	0.0605	0.3198	0.00396	0.08508	0.00115
OBD1-20	0.10819	0.00116	4.73988	0.05618	0.31779	0.0037	0.08367	0.00099

Table 2.

Sample No.	Drillhole	Sm (ppm)	Nd (ppm)	147Sm/144Nd	143Nd/144Nd	$\varepsilon_{Nd(0)a}$	$\varepsilon_{Nd(T)}$	T_{DM} (Ga)
R1643391	OBD 11	5.7	31.7	0.1080	0.511493	-22.3	-3.0	2.36
R1643397	OBD 7	8.9	56.5	0.0955	0.511284	-26.4	-4.4	2.38
R1633400	OBD 8	7.4	40.5	0.1111	0.511431	-23.6	-4.9	2.52
R1633403	OBD 9	9.0	51.9	0.1052	0.511336	-25.4	-5.5	2.31
R1633406	MANYA 4	3.9	21.5	0.1096	0.511359	-24.9	-6.0	2.59
R1633427	MIDDLE BORE 1	2.7	10.5	0.1553	0.512354	-5.5	3.5	2.04
R1633428	MIDDLE BORE 1	4.0	14.8	0.1650	0.512451	-3.7	3.3	2.14
R1633444	OBD 5	6.4	45.0	0.0855	0.511267	-26.8	-2.5	2.22
R1633450	OBD 3	10.2	55.9	0.1099	0.511463	-22.9	-4.0	2.45
R1633452	OBD 1	8.3	43.7	0.1143	0.511489	-22.4	-4.5	2.51

Table 3.

Spot No.	207Pb/206Pb	1σ	207Pb/235U	1σ	206Pb/238U	1σ	207Pb/206Pb (Ma)	1σ	207Pb/235U (Ma)	1σ	206Pb/238U (Ma)	1σ	Concordancy %
						OBD 6							
m396_1	0.10426	0.00104	4.39846	0.05712	0.30527	0.00408	1701.4	18.32	1712.1	10.74	1717.4	20.14	100
m396_2	0.10062	0.00104	4.35102	0.05756	0.31292	0.00421	1635.5	19.12	1703.1	10.92	1755.1	20.65	97
m396_3	0.10797	0.00109	4.53378	0.0591	0.30386	0.00407	1765.4	18.36	1737.2	10.84	1710.4	20.1	102
m396_4	0.10967	0.00116	4.39544	0.05867	0.29003	0.00392	1793.9	19.18	1711.5	11.04	1641.7	19.56	104
m396_5	0.10796	0.00107	4.43367	0.05739	0.29719	0.00399	1765.2	17.96	1718.7	10.72	1677.4	19.85	102
m396_6	0.1087	0.00107	4.35429	0.05613	0.28988	0.00389	1777.6	17.93	1703.7	10.64	1640.9	19.46	104
m396_7	0.1069	0.00108	4.34861	0.05688	0.29441	0.00398	1747.2	18.32	1702.6	10.8	1663.5	19.82	102
m396_8	0.10096	0.00102	4.26593	0.05589	0.30577	0.00414	1641.8	18.7	1686.8	10.78	1719.9	20.45	98
m396_9	0.10243	0.00101	4.37592	0.05667	0.30918	0.00419	1668.7	18.21	1707.8	10.7	1736.7	20.61	98
m396_10	0.10204	0.00102	4.25378	0.05557	0.30171	0.0041	1661.6	18.4	1684.5	10.74	1699.8	20.33	99
m396_11	0.10008	0.00099	4.17117	0.05429	0.30166	0.00411	1625.6	18.3	1668.4	10.66	1699.5	20.36	98
m396_12	0.10071	0.001	4.25859	0.05579	0.30615	0.00423	1637.3	18.41	1685.4	10.77	1721.7	20.89	98
m396_13	0.09599	0.00103	4.53473	0.06252	0.34183	0.00478	1547.5	20.12	1737.4	11.47	1895.5	22.96	92
m396_14	0.10395	0.001	4.26117	0.05495	0.29675	0.0041	1695.8	17.68	1685.9	10.61	1675.2	20.4	101
m396_15	0.10498	0.001	4.32764	0.05573	0.29842	0.00412	1713.9	17.36	1698.6	10.62	1683.5	20.47	101
m396_16	0.10598	0.00105	4.28304	0.05653	0.29247	0.00408	1731.4	18.02	1690.1	10.86	1653.9	20.35	102
m396_17	0.10604	0.00104	4.26263	0.05595	0.29097	0.00405	1732.4	17.92	1686.2	10.8	1646.4	20.2	102
m396_19	0.10088	0.00102	4.10252	0.05489	0.2943	0.0041	1640.4	18.6	1654.8	10.92	1663	20.43	100
m396_20	0.10039	0.00097	4.32281	0.05671	0.31163	0.00432	1631.3	17.9	1697.7	10.82	1748.7	21.24	97
m396_21	0.10369	0.00109	4.27148	0.05835	0.29817	0.00415	1691.2	19.32	1687.9	11.24	1682.2	20.62	100
m396_22	0.10116	0.001	4.14911	0.05472	0.29688	0.0041	1645.5	18.25	1664	10.79	1675.8	20.38	99
m396_23	0.10083	0.00103	4.27041	0.05738	0.30647	0.00424	1639.5	18.82	1687.7	11.05	1723.3	20.93	98
m396_24	0.0961	0.00095	3.68399	0.04877	0.27741	0.00383	1549.8	18.47	1567.9	10.57	1578.3	19.32	99
m396_25	0.10842	0.00108	4.45754	0.05916	0.29753	0.00409	1772.9	18.05	1723.1	11.01	1679	20.32	103
m396_26	0.1028	0.00104	4.25557	0.05685	0.2996	0.00412	1675.2	18.55	1684.8	10.98	1689.3	20.43	100
m396_27	0.10286	0.00107	4.17755	0.05631	0.29406	0.00402	1676.4	19.11	1669.6	11.04	1661.8	20.03	100

Spot No.	207Pb/206Pb	1σ	207Pb/235U	1σ	206Pb/238U	1σ	207Pb/206Pb (Ma)	1σ	207Pb/235U (Ma)	1σ	206Pb/238U (Ma)	1σ	Concordancy %
						OBD 9							
m405_1	0.08734	0.00087	3.09377	0.03996	0.25691	0.0035	1368	19.06	1431.1	9.91	1474	17.95	97
m405_2	0.09184	0.00095	3.20774	0.04222	0.25315	0.00347	1464	19.5	1459	10.19	1454.7	17.86	100
m405_3	0.0905	0.00091	3.31473	0.04311	0.26563	0.00364	1436	18.98	1484.5	10.15	1518.6	18.54	98
m405_4	0.09105	0.00092	3.18534	0.04147	0.25374	0.00348	1447.6	19.06	1453.6	10.06	1457.7	17.9	100
m405_5	0.08828	0.0009	3.565	0.04615	0.2932	0.00401	1388.7	19.31	1541.8	10.26	1657.5	19.97	93
m405_6	0.08843	0.00087	3.23851	0.04108	0.2656	0.00361	1391.9	18.67	1466.4	9.84	1518.4	18.37	97
m405_7	0.09053	0.00092	3.04978	0.03947	0.24439	0.00332	1436.7	19.35	1420.2	9.9	1409.5	17.2	101
m405_8	0.08981	0.00088	3.03001	0.03766	0.24459	0.00326	1421.3	18.56	1415.2	9.49	1410.5	16.9	100
m843_1	0.09654	0.00107	4.31063	0.05911	0.32336	0.00432	1558.2	20.73	1695.4	11.3	1806.1	21.04	94
m843_2	0.09423	0.00104	4.74106	0.06533	0.36494	0.00495	1512.7	20.72	1774.5	11.55	2005.6	23.37	88
m843_3	0.09578	0.00098	4.36434	0.0569	0.33	0.00436	1543.4	19.06	1705.6	10.77	1838.4	21.12	93
m843_4	0.09188	0.00096	4.41728	0.05889	0.34865	0.00469	1464.8	19.78	1715.6	11.04	1928.2	22.41	89
m843_5	0.09169	0.00095	4.53346	0.06025	0.35869	0.00484	1460.8	19.65	1737.1	11.06	1975.9	22.95	88
m843_6	0.09424	0.00095	4.36418	0.05689	0.33562	0.00449	1512.9	18.94	1705.6	10.77	1865.5	21.65	91
m843_7	0.09439	0.001	3.29598	0.04341	0.25286	0.00329	1516	19.82	1480.1	10.26	1453.2	16.93	102
m843_8	0.08923	0.00089	3.95562	0.05144	0.32111	0.00433	1409.1	18.93	1625.1	10.54	1795.2	21.11	91
m843_9	0.10314	0.00112	5.02762	0.06859	0.35335	0.00483	1681.3	19.85	1824	11.56	1950.6	22.99	94
m843_10	0.09659	0.00101	4.32667	0.05814	0.3244	0.00444	1559.3	19.47	1698.5	11.08	1811.2	21.61	94
m843_11	0.09034	0.00093	4.33485	0.05752	0.34732	0.00472	1432.7	19.45	1700	10.95	1921.8	22.59	88
m843_12	0.08682	0.00092	3.7256	0.05004	0.31025	0.00429	1356.6	20.36	1576.9	10.75	1741.9	21.09	91
m843_13	0.09047	0.00106	3.50009	0.04989	0.27977	0.00395	1435.3	22.25	1527.2	11.26	1590.2	19.89	96
m843_14	0.0929	0.00093	3.74919	0.04902	0.29187	0.00403	1485.6	19.07	1581.9	10.48	1650.8	20.12	96
m843_15	0.09099	0.00087	3.70097	0.0471	0.2942	0.00407	1446.2	18.01	1571.6	10.17	1662.5	20.26	95
m843_16	0.08911	0.00095	4.17617	0.05662	0.33908	0.00476	1406.5	20.31	1669.4	11.11	1882.3	22.9	89

Spot No.	207Pb/206Pb	1σ	207Pb/235U	1σ	206Pb/238U	1σ	207Pb/206Pb (Ma)	1σ	207Pb/235U (Ma)	1σ	206Pb/238U (Ma)	1σ	Concordancy %
						OBD 12							
m412a_1	0.10268	0.00116	4.07731	0.05455	0.28711	0.00377	1673.2	20.78	1649.8	10.91	1627.1	18.91	101
m412a_2	0.10148	0.00115	4.17652	0.05597	0.29769	0.00392	1651.3	20.79	1669.4	10.98	1679.8	19.47	99
m412a_3	0.10272	0.00125	4.2891	0.06033	0.30218	0.00402	1673.8	22.37	1691.3	11.58	1702.1	19.9	99
m412a_4	0.09998	0.00122	3.73561	0.05237	0.27012	0.00359	1623.7	22.49	1579	11.23	1541.4	18.21	102
m412a_5	0.10213	0.00119	4.2223	0.05778	0.29901	0.00396	1663.2	21.43	1678.4	11.23	1686.4	19.65	100
m412a_6	0.10313	0.00118	4.16266	0.05605	0.29195	0.00385	1681.2	20.93	1666.7	11.02	1651.3	19.19	101
m412a_7	0.09454	0.00098	3.4707	0.04451	0.26553	0.00347	1518.8	19.45	1520.6	10.11	1518.1	17.65	100
m412a_8	0.09682	0.00109	3.70941	0.04962	0.27708	0.00364	1563.7	20.97	1573.4	10.7	1576.6	18.36	100
m412a_9	0.10232	0.00105	4.15601	0.05327	0.29372	0.00385	1666.7	18.91	1665.4	10.49	1660.1	19.18	100
m412a_10	0.10445	0.00113	4.24431	0.05564	0.29391	0.00385	1704.6	19.82	1682.6	10.77	1661.1	19.17	101
m412a_11	0.09198	0.00097	3.29871	0.0429	0.25937	0.0034	1466.9	19.8	1480.7	10.13	1486.6	17.41	100
m412a_12	0.10398	0.00107	4.27718	0.05459	0.29749	0.00388	1696.4	18.91	1689	10.5	1678.8	19.28	101
m412a_13	0.10466	0.00114	4.33021	0.05708	0.29929	0.00394	1708.3	19.86	1699.1	10.87	1687.8	19.55	101
m412a_14	0.1022	0.00112	4.17015	0.05539	0.2951	0.0039	1664.5	20.08	1668.2	10.88	1667	19.41	100
m412a_15	0.09845	0.00113	3.83179	0.05261	0.28179	0.0038	1595	21.36	1599.4	11.06	1600.4	19.1	100
m412a_16	0.09656	0.00101	3.83543	0.0503	0.28741	0.00388	1558.8	19.45	1600.2	10.56	1628.6	19.42	98
m412a_17	0.09926	0.00107	3.81949	0.05116	0.27834	0.00379	1610.2	19.98	1596.9	10.78	1583	19.1	101
m412a_18	0.09731	0.00099	3.55441	0.0461	0.26423	0.00358	1573.2	18.86	1539.4	10.28	1511.4	18.23	102
m412a_19	0.10677	0.0011	4.36341	0.05683	0.29564	0.00399	1745	18.76	1705.4	10.76	1669.6	19.87	102
m412a_20	0.096	0.001	3.50302	0.04581	0.26408	0.00355	1547.8	19.47	1527.9	10.33	1510.7	18.12	101
m412a_21	0.09576	0.00095	3.53128	0.04543	0.2668	0.00361	1543	18.59	1534.2	10.18	1524.5	18.35	101
m412a_22	0.09686	0.00102	3.50332	0.04562	0.2619	0.00348	1564.6	19.65	1528	10.29	1499.5	17.77	102
m412a_23	0.09957	0.00099	3.83219	0.04917	0.27838	0.00376	1616.1	18.36	1599.5	10.33	1583.2	18.95	101
m412a_24	0.10646	0.00129	4.21544	0.0599	0.28659	0.00391	1739.7	22.07	1677	11.66	1624.5	19.59	103
m412a_25	0.09671	0.001	3.66326	0.04754	0.27416	0.00366	1561.7	19.32	1563.4	10.35	1561.9	18.5	100
m412a_26	0.10506	0.00111	4.2804	0.05644	0.29498	0.00386	1715.4	19.33	1689.6	10.85	1666.4	19.23	101
m412a_27	0.10114	0.00134	3.94199	0.05842	0.28239	0.00374	1645.2	24.43	1622.3	12	1603.4	18.78	101
m412a_28	0.10551	0.00117	4.34219	0.05858	0.29798	0.0039	1723.3	20.27	1701.4	11.13	1681.3	19.39	101
m412a_29	0.10567	0.00109	4.42756	0.05767	0.30335	0.00397	1726	18.82	1717.5	10.79	1707.9	19.63	101
m412a_30	0.10772	0.00112	4.5131	0.05976	0.3034	0.00403	1761.2	18.79	1733.4	11.01	1708.1	19.95	101
m412a_31	0.1044	0.00109	4.36336	0.05707	0.30259	0.00394	1703.8	19.17	1705.4	10.8	1704.1	19.52	100
m412a_32	0.10403	0.00111	4.36474	0.05783	0.30376	0.00398	1697.3	19.56	1705.7	10.95	1709.9	19.66	100
m412a_33	0.10225	0.00125	4.26759	0.06048	0.30225	0.00397	1665.3	22.45	1687.1	11.66	1702.4	19.67	99

Spot No.	207Pb/206Pb	1σ	207Pb/235U	1σ	206Pb/238U	1σ	207Pb/206Pb (Ma)	1σ	207Pb/235U (Ma)	1σ	206Pb/238U (Ma)	1σ	Concordancy %
						OBD 12 (cont)							
m412a_34	0.10444	0.00122	4.35567	0.06109	0.30199	0.00402	1704.4	21.39	1704	11.58	1701.2	19.92	100
m412a_35	0.10321	0.00148	4.26703	0.06789	0.29939	0.00411	1682.6	26.28	1687	13.09	1688.3	20.39	100
m412a_36	0.10024	0.00099	4.17357	0.05364	0.30169	0.00409	1628.5	18.22	1668.8	10.53	1699.7	20.24	98
m412a_37	0.10015	0.00098	4.33919	0.05556	0.31395	0.00425	1626.8	18.09	1700.8	10.57	1760.1	20.85	97
m412a_38	0.10266	0.00112	4.44598	0.06019	0.31381	0.00431	1672.7	19.97	1720.9	11.22	1759.4	21.13	98
m412a_39	0.10518	0.00114	4.39213	0.05931	0.30257	0.00415	1717.4	19.78	1710.9	11.17	1704	20.54	100
m412a_40	0.10098	0.00104	4.15942	0.0546	0.29847	0.00406	1642.1	18.94	1666.1	10.74	1683.7	20.17	99
m412a_41	0.09976	0.00103	3.90113	0.05146	0.28336	0.00386	1619.5	19.18	1613.9	10.66	1608.2	19.39	100
m412a_42	0.09602	0.00101	3.58476	0.04762	0.27051	0.00369	1548.1	19.6	1546.2	10.55	1543.4	18.72	100
m412a_43	0.09578	0.00099	3.76352	0.0497	0.28471	0.00388	1543.4	19.4	1585	10.6	1615.1	19.46	98
m412a_44	0.10429	0.00105	4.16853	0.05414	0.28961	0.00393	1701.9	18.43	1667.9	10.64	1639.6	19.66	102
m412a_45	0.09759	0.00101	4.07017	0.05376	0.30219	0.00412	1578.6	19.31	1648.3	10.77	1702.2	20.39	97
m412a_46	0.09665	0.00099	3.56734	0.04686	0.26743	0.00364	1560.5	19.17	1542.3	10.42	1527.7	18.51	101
m412a_47	0.09631	0.00096	3.78196	0.04884	0.28454	0.00386	1553.7	18.57	1588.9	10.37	1614.2	19.36	98
m412a_48	0.10456	0.00109	4.22291	0.0558	0.29263	0.00399	1706.6	19.04	1678.5	10.85	1654.7	19.91	101
m739_1	0.10497	0.00109	4.42559	0.06572	0.30517	0.00456	1713.8	18.89	1717.1	12.3	1716.9	22.54	100
m739_2	0.10425	0.00105	4.33355	0.06302	0.3009	0.00444	1701.1	18.51	1699.8	12	1695.8	21.99	100
m739_3	0.10328	0.00105	4.54702	0.06656	0.31869	0.00472	1683.8	18.63	1739.6	12.18	1783.3	23.08	98
m739_4	0.10478	0.00104	4.60574	0.06664	0.3182	0.00469	1710.4	18.18	1750.3	12.07	1780.9	22.94	98
m739_5	0.1037	0.00123	4.31272	0.06725	0.30109	0.00451	1691.3	21.69	1695.8	12.85	1696.7	22.36	100
m739_6	0.10574	0.00107	4.30618	0.06275	0.29477	0.00436	1727.1	18.45	1694.5	12.01	1665.3	21.71	102
m739_7	0.10183	0.00105	4.25166	0.06235	0.30223	0.00446	1657.8	19.01	1684.1	12.05	1702.4	22.1	99
m739_8	0.11271	0.00113	4.25224	0.06164	0.27311	0.00402	1843.5	18.09	1684.2	11.92	1556.6	20.37	108
m739_9d	0.10454	0.00107	4.37821	0.06397	0.30317	0.00448	1706.2	18.65	1708.2	12.08	1707	22.18	100
m739_10	0.10823	0.00117	4.44031	0.06603	0.29705	0.00439	1769.7	19.61	1719.9	12.32	1676.7	21.8	103
m739_11	0.10599	0.00128	4.21195	0.04826	0.2877	0.00123	1731.5	22.06	1676.4	9.4	1630	6.17	103
m739_12	0.10409	0.00116	4.37956	0.04622	0.30461	0.00121	1698.2	20.41	1708.5	8.72	1714.1	5.96	100
m739_13	0.09763	0.00155	3.47007	0.0522	0.25733	0.00143	1579.3	29.44	1520.4	11.86	1476.1	7.35	103
m739_14	0.1147	0.00117	4.43575	0.04266	0.27996	0.00101	1875.2	18.22	1719	7.97	1591.2	5.08	108
m739_15	0.10724	0.00114	3.78167	0.03789	0.25529	0.00095	1753	19.18	1588.9	8.04	1465.7	4.88	108
m739_16	0.10997	0.00116	4.03547	0.04032	0.26566	0.00099	1798.9	19.11	1641.4	8.13	1518.7	5.06	108
m739_17	0.11129	0.00115	4.01736	0.0392	0.26133	0.00095	1820.6	18.6	1637.7	7.93	1496.6	4.84	109

Spot No.	207Pb/206Pb	1σ	207Pb/235U	1σ	206Pb/238U	1σ	207Pb/206Pb (Ma)	1σ	207Pb/235U (Ma)	1σ	206Pb/238U (Ma)	1σ	Concordancy %
						OBD 12 (cont)							
m739_18	0.11496	0.00119	4.39072	0.04288	0.2765	0.00101	1879.3	18.49	1710.6	8.08	1573.7	5.09	109
m739_19	0.11156	0.00112	4.13596	0.03938	0.2684	0.00095	1825	18.14	1661.4	7.79	1532.7	4.83	108
m739_20	0.11083	0.00105	4.19168	0.03769	0.27381	0.0009	1813	17.14	1672.4	7.37	1560.1	4.56	107
m739_21	0.10323	0.00112	3.54088	0.03624	0.24832	0.00094	1683	19.83	1536.4	8.1	1429.8	4.84	107
m739_22	0.10187	0.00104	4.22058	0.05998	0.2939	0.00427	1658.5	18.82	1678	11.67	1661	21.26	101
m739_23	0.10415	0.00108	4.41518	0.0631	0.30073	0.00437	1699.3	18.96	1715.2	11.83	1694.9	21.68	101
m739_24	0.10184	0.00103	4.14363	0.05861	0.28862	0.00419	1657.9	18.62	1663	11.57	1634.6	20.94	102
m739_25	0.10174	0.00103	4.29062	0.06079	0.29917	0.00434	1656	18.7	1691.6	11.67	1687.2	21.54	100
m739_26	0.1034	0.00116	4.26002	0.06317	0.29225	0.00429	1686	20.54	1685.7	12.19	1652.8	21.4	102
m739_27	0.09921	0.00126	4.16184	0.06585	0.29758	0.00444	1609.3	23.45	1666.5	12.95	1679.3	22.06	99
m739_28	0.09521	0.00098	3.68712	0.05265	0.2747	0.00399	1532.3	19.33	1568.6	11.41	1564.6	20.18	100
m739_29	0.10337	0.00105	4.45625	0.06325	0.30581	0.00444	1685.4	18.71	1722.9	11.77	1720.1	21.92	100
m739_30	0.10197	0.00105	4.52126	0.06454	0.31453	0.00457	1660.2	19	1734.9	11.87	1763	22.42	98
m739_31	0.10501	0.00108	4.44234	0.0632	0.3001	0.00436	1714.4	18.74	1720.3	11.79	1691.8	21.62	102
m739_32	0.09162	0.00095	3.37395	0.04828	0.26124	0.00379	1459.3	19.61	1498.4	11.21	1496.2	19.4	100
m739_33	0.09609	0.00105	3.43866	0.05254	0.25921	0.00395	1549.5	20.38	1513.3	12.02	1485.8	20.25	102
m739_34	0.10349	0.00112	4.38074	0.06674	0.30666	0.00469	1687.6	19.84	1708.7	12.6	1724.2	23.12	99
m739_35	0.10475	0.00114	4.26477	0.06401	0.29456	0.00442	1709.9	19.91	1686.6	12.35	1664.3	22.02	101
m739_36	0.10408	0.00109	4.15666	0.06242	0.28909	0.00441	1698.1	19.13	1665.5	12.29	1637	22.08	102
m739_37	0.10565	0.00109	4.38065	0.06522	0.30034	0.00456	1725.6	18.83	1708.7	12.31	1693	22.59	101
m739_38	0.10495	0.00105	4.41915	0.06542	0.30476	0.00465	1713.4	18.22	1715.9	12.26	1714.9	22.98	100
m739_39	0.0989	0.00101	3.937	0.05893	0.2884	0.00441	1603.4	18.98	1621.3	12.12	1633.5	22.08	99

Table 4.

OBD1 - #3451	g	opx	cpx	ilm	plag	hbd
SiO2	37.47	49.70	49.77	0.03	56.45	40.42
TiO2	0.06	0.07	0.18	48.83	0.00	2.26
Al2O3	20.54	0.70	2.16	0.00	25.90	11.38
Cr2O3	0.00	0.00	0.03	0.02	0.00	0.01
FeO	30.85	12.53	47.14	27.49	0.09	17.98
MnO	1.72	0.69	0.37	0.36	0.02	0.16
MgO	4.04	15.80	11.24	0.16	0.02	9.02
CaO	6.97	0.63	21.80	0.02	8.95	11.66
Na2O	0.02	0.00	0.38	0.00	6.46	1.28
K2O	0.00	0.00	0.01	0.00	0.30	1.96
Totals	98.36	98.55	98.81	96.98	98.20	96.30
Oxygens	12	6	6	3	8	23
Si	3.007	1.965	1.912	0.001	2.582	6.254
Ti	0.004	0.002	0.005	0.957	0.000	0.263
Al	1.943	0.033	0.098	0.000	1.397	2.077
Cr	0.000	0.000	0.001	0.000	0.000	0.002
Fe3	0.039	0.034	0.095	0.084	0.003	0.209
Fe2	1.806	0.986	0.307	0.943	0.000	2.117
Mn	0.117	0.023	0.012	0.008	0.001	0.020
Mg	0.484	0.931	0.643	0.006	0.001	2.080
Ca	0.599	0.027	0.897	0.000	0.439	1.933
Na	0.002	0.000	0.028	0.000	0.573	0.383
K	0.000	0.000	0.001	0.000	0.017	0.387
Sum	8.000	4.000	4.000	2.000	5.013	15.724

OBD1 - #3456	g	opx	cpx	ilm	plag	hbd
SiO2	36.91	49.60	50.00	0.01	55.76	40.54
TiO2	0.06	0.04	0.20	50.25	0.00	1.56
Al2O3	21.30	1.10	2.23	0.00	26.96	11.67
Cr2O3	0.07	0.03	0.02	0.00	0.01	0.05
FeO	27.79	31.55	13.09	45.59	0.00	18.59
MnO	1.57	0.58	0.35	0.57	0.00	0.14
MgO	4.25	15.45	11.22	0.48	0.00	9.26
CaO	7.01	0.65	21.78	0.03	9.60	11.56
Na2O	0.01	0.01	0.38	0.00	6.07	1.15
K2O	0.01	0.00	0.00	0.00	0.28	1.93
Totals	99.18	99.15	99.63	97.13	98.76	96.89
Oxygens	12	6	6	3	8	23
Si	2.936	1.953	1.908	0.000	2.540	6.220
Ti	0.004	0.001	0.006	0.980	0.000	0.180
Al	1.998	0.051	0.100	0.000	1.447	2.111
Cr	0.004	0.001	0.001	0.000	0.000	0.006
Fe3	0.120	0.040	0.100	0.041	0.003	0.487
Fe2	1.729	0.999	0.318	0.948	0.000	1.898
Mn	0.106	0.019	0.011	0.012	0.000	0.019
Mg	0.503	0.907	0.638	0.019	0.000	2.118
Ca	0.598	0.027	0.890	0.001	0.469	1.900
Na	0.001	0.001	0.028	0.000	0.536	0.343
K	0.001	0.000	0.000	0.000	0.016	0.379
Sum	8.000	4.000	4.000	2.000	5.011	15.659

Middle Bore - #3438	g	cpx	mt	plag	hbd
SiO2	36.65	49.52	0.07	55.66	41.12
TiO2	0.06	0.13	0.16	0.01	1.42
Al2O3	20.81	1.78	0.29	26.97	11.24
Cr2O3	0.02	0.01	0.04	0.00	0.01
FeO	28.22	15.60	91.30	0.02	19.19
MnO	1.98	0.34	0.01	0.00	0.17
MgO	4.04	10.50	0.02	0.02	9.02
CaO	7.16	20.55	0.00	9.95	11.58
Na2O	0.00	0.27	0.00	5.98	1.25
K2O	0.00	0.00	0.00	0.24	1.52
Totals	99.25	99.02	98.62	98.86	96.95
Oxygens	12	6	4	8	23
Si	2.926	1.919	0.003	2.534	6.300
Ti	0.003	0.004	0.005	0.000	0.163
Al	1.959	0.081	0.013	1.448	2.031
Cr	0.001	0.000	0.001	0.000	0.001
Fe3	0.182	0.094	1.970	0.001	0.500
Fe2	1.702	0.411	1.006	0.000	1.958
Mn	0.134	0.011	0.000	0.000	0.022
Mg	0.481	0.606	0.001	0.001	2.060
Ca	0.612	0.853	0.000	0.486	1.901
Na	0.000	0.020	0.000	0.528	0.371
K	0.000	0.000	0.000	0.014	0.297
Sum	8.000	4.000	3.000	5.012	15.604

Mt Furner - #3411	g	bi	mu	plag	K-spar
SiO2	35.86	35.26	46.51	64.21	64.97
TiO2	0.02	1.81	0.02	0.03	0.00
Al2O3	20.93	19.09	35.71	20.62	18.31
Cr2O3	0.07	0.00	0.01	0.00	0.00
FeO	29.68	21.42	1.92	0.02	0.00
MnO	9.00	0.40	0.02	0.03	0.00
MgO	3.15	7.75	0.56	0.00	0.02
CaO	0.50	0.06	0.00	1.71	0.02
Na2O	0.03	0.16	0.30	10.57	1.39
K2O	0.00	9.27	10.49	0.20	14.89
Totals	99.49	95.23	95.54	97.39	99.65
Oxygens	12	11	11	8	8
Si	2.917	2.713	3.089	2.899	3.000
Ti	0.001	0.105	0.001	0.001	0.000
Al	2.007	1.732	2.795	1.097	0.997
Cr	0.005	0.000	0.000	0.000	0.000
Fe3	0.157	0.000	0.000	0.001	0.001
Fe2	1.863	1.378	0.107	0.000	0.000
Mn	0.620	0.026	0.001	0.001	0.000
Mg	0.382	0.889	0.055	0.000	0.001
Ca	0.043	0.005	0.000	0.083	0.001
Na	0.005	0.024	0.038	0.926	0.125
K	0.000	0.911	0.890	0.011	0.878
Sum	8.000	7.783	6.977	5.019	5.003

Manya4 - #3408	g	bi	ilm	plag
SiO2	36.54	34.49	0.04	58.86
TiO2	0.04	3.83	47.70	0.00
Al2O3	21.09	17.27	0.00	24.27
Cr2O3	0.06	0.08	0.33	0.01
FeO	32.61	20.54	45.67	0.07
MnO	2.85	0.16	0.26	0.05
MgO	4.78	9.02	0.00	0.00
CaO	1.29	0.01	0.02	6.17
Na2O	0.03	0.09	0.03	8.30
K2O	0.00	9.14	0.01	0.22
Totals	99.54	94.64	94.43	97.95
Oxygens	12	11	3	8
Si	2.931	2.670	0.001	2.682
Ti	0.003	0.223	0.961	0.000
Al	1.994	1.577	0.000	1.304
Cr	0.004	0.005	0.007	0.000
Fe3	0.140	0.000	0.072	0.003
Fe2	2.048	1.330	0.950	0.000
Mn	0.194	0.010	0.006	0.002
Mg	0.571	1.041	0.000	0.000
Ca	0.111	0.001	0.001	0.301
Na	0.005	0.014	0.002	0.733
K	0.000	0.904	0.001	0.013
Sum	8.000	7.775	2.000	5.038

OBD3 -#3413	g	mt	plag	hbd
SiO2	36.25	0.01	55.64	40.63
TiO2	0.04	0.08	0.00	1.42
Al2O3	20.62	0.28	24.48	11.45
Cr2O3	0.00	0.05	0.01	0.03
FeO	25.51	90.60	0.09	19.69
MnO	4.63	0.06	0.00	0.63
MgO	3.74	0.01	0.01	7.80
CaO	7.34	0.00	7.64	11.43
Na2O	0.01	0.00	6.83	1.11
K2O	0.00	0.02	0.58	1.61
Totals	98.47	101.09	95.32	96.24
Oxygens	12	3	8	23
Si	2.920	0.000	2.620	6.303
Ti	0.002	0.002	0.000	0.166
Al	1.959	0.009	1.359	2.094
Cr	0.000	0.001	0.000	0.003
Fe3	0.199	1.973	0.004	0.494
Fe2	1.519	0.020	0.000	2.060
Mn	0.316	0.001	0.000	0.083
Mg	0.449	0.000	0.001	1.802
Ca	0.634	0.000	0.386	1.901
Na	0.002	0.000	0.624	0.333
K	0.000	0.001	0.035	0.320
Sum	8.000	2.007	5.028	15.561

OBD7 -#3398	g	bi	K-spar	plag	mt
SiO2	36.93	36.96	63.70	58.29	0.00
TiO2	0.03	3.19	0.01	0.01	0.11
Al2O3	20.82	15.65	19.14	24.94	0.07
Cr2O3	0.00	0.04	0.00	0.00	0.05
FeO	22.37	23.20	0.01	0.10	90.08
MnO	8.76	0.33	0.00	0.00	0.02
MgO	0.88	7.69	0.00	0.00	0.00
CaO	8.83	0.06	0.01	6.86	0.05
Na2O	0.00	0.07	0.91	7.71	0.07
K2O	0.00	8.23	14.25	0.13	0.01
Totals	98.63	95.42	98.05	98.04	97.18
Oxygens	12	11	8	8	4
Si	3.002	2.844	2.975	2.654	0.000
Ti	0.002	0.184	0.000	0.000	0.003
Al	1.995	1.420	1.054	1.339	0.003
Cr	0.000	0.002	0.000	0.000	0.002
Fe3	0.000	0.000	0.000	0.003	1.995
Fe2	1.521	1.493	0.000	0.000	0.988
Mn	0.603	0.021	0.000	0.000	0.001
Mg	0.107	0.882	0.000	0.000	0.000
Ca	0.769	0.005	0.001	0.335	0.002
Na	0.000	0.011	0.083	0.680	0.006
K	0.000	0.808	0.850	0.008	0.001
Sum	7.999	7.670	4.963	5.019	3.000

OBD9 -#3404	gt	bi	plag
SiO2	36.79	35.10	55.45
TiO2	0.01	4.03	0.00
Al2O3	20.48	15.93	26.38
Cr2O3	0.04	0.04	0.01
FeO	32.57	19.70	0.04
MnO	2.80	0.06	0.00
MgO	4.76	10.46	0.00
CaO	1.88	0.00	9.74
Na2O	0.04	0.08	6.19
K2O	0.00	9.53	0.21
Totals	99.64	94.95	98.02
Oxygens	12	11	8
Si	2.950	2.705	2.547
Ti	0.000	0.233	0.000
Al	1.936	1.447	1.428
Cr	0.002	0.003	0.000
Fe3	0.165	0.000	0.002
Fe2	2.019	1.270	0.000
Mn	0.190	0.004	0.000
Mg	0.569	1.201	0.000
Ca	0.162	0.000	0.479
Na	0.006	0.012	0.552
K	0.000	0.938	0.012
Sum	8.000	7.812	5.020

OBD9 -#3405	gt	bi	plag
SiO2	37.72	35.55	58.63
TiO2	0.02	3.86	0.00
Al2O3	21.57	17.42	25.87
Cr2O3	0.02	0.06	0.00
FeO	32.34	18.75	0.03
MnO	2.64	0.07	0.02
MgO	5.31	10.27	0.00
CaO	1.43	0.00	7.80
Na2O	0.03	0.10	7.23
K2O	0.00	8.24	0.29
Totals	101.24	94.34	99.86
Oxygens	12	11	8
Si	2.959	2.712	2.626
Ti	0.001	0.221	0.000
Al	1.995	1.566	1.366
Cr	0.001	0.004	0.000
Fe3	0.088	0.000	0.001
Fe2	2.034	1.196	0.000
Mn	0.175	0.005	0.001
Mg	0.621	1.168	0.000
Ca	0.120	0.000	0.374
Na	0.005	0.015	0.628
K	0.000	0.803	0.016
Sum	8.000	7.690	5.013

OBD6	g	bi	plag	ilm
SiO2	36.26	33.88	58.35	0.36
TiO2	0.05	4.43	0.01	57.74
Al2O3	21.08	14.02	24.70	0.03
Cr2O3	0.02	0.03	0.00	0.00
FeO	33.44	26.40	0.07	35.76
MnO	2.06	0.07	0.03	0.55
MgO	2.29	6.72	0.00	0.03
CaO	5.14	0.00	7.40	0.10
Na2O	0.01	0.04	7.46	0.02
K2O	0.00	9.38	0.35	0.00
Totals	100.67	95.00	98.37	94.59
Oxygens	12	11	8	3
Si	2.906	2.711	2.654	0.009
Ti	0.003	0.267	0.000	1.103
Al	1.992	1.322	1.324	0.001
Cr	0.001	0.002	0.000	0.000
Fe3	0.190	0.000	0.003	0.000
Fe2	2.052	1.767	0.000	0.759
Mn	0.140	0.005	0.001	0.012
Mg	0.273	0.802	0.000	0.001
Ca	0.441	0.000	0.361	0.003
Na	0.002	0.007	0.658	0.001
K	0.000	0.959	0.020	0.000
Sum	8.000	7.842	5.021	1.888

Table 5.

Drillhole name	Drillhole Number	Unit 1		Unit 2		Unit 3		Unit 4		Unit 5		Unit 6		Unit 7		Unit 8	
		From (m)	To (m)	From (m)	To (m)	From (m)	To (m)	From (m)	To (m)	From (m)	To (m)	From (m)	To (m)	From (m)	To (m)	From (m)	To (m)
OBD 1	1582	0.00	63.50	63.50	115.30	115.30	140.00	-	-	-	-	-	-	-	-	-	-
OBD 3	1051	0.00	24.00	24.00	26.00	26.00	40.00	40.00	123.00	123.00	218.00	-	-	-	-	-	-
OBD 5	1583	0.00	52.00	52.00	131.80	131.80	134.10	-	-	-	-	-	-	-	-	-	-
OBD 6	1586	0.00	2.00	2.00	8.00	8.00	32.00	32.00	47.00	47.00	243.80	243.80	251.10	-	-	-	-
OBD 7	1588	0.00	61.00	61.00	116.00	116.00	260.40	260.40	269.60	-	-	-	-	-	-	-	-
OBD 8	1577	0.00	66.30	66.30	175.20	175.20	185.00	-	-	-	-	-	-	-	-	-	-
OBD 9	1592	0.00	67.50	67.50	170.00	170.00	248.00	248.00	389.00	389.00	400.70	-	-	-	-	-	-
OBD 11	1037	0.00	56.80	56.80	115.70	115.70	223.70	223.70	232.70	-	-	-	-	-	-	-	-
OBD 12	1040	0.00	18.00	18.00	88.00	88.00	463.40	463.40	474.40	-	-	-	-	-	-	-	-
Lake Maurice East 1	476	0.00	691.00	691.00	722.38	-	-	-	-	-	-	-	-	-	-	-	-
Mount Turner 1	5145	0.00	60.96	60.96	105.16	105.15	132.59	132.59	521.21	521.21	548.64	548.64	555.04	-	-	-	-
Manya 4	3583	0.00	14.00	14.00	32.00	32.00	106.00	106.00	162.00	162.00	406.00	406.00	498.00	498.80	796.00	796.00	806.70
Middle Bore 1	3615	0.00	44.00	44.00	160.00	160.00	371.00	371.00	557.60	-	-	-	-	-	-	-	-

Table 6.

Sample No.	Drill hole name	Interval (m) From	To	Petrography of selected slides
R1643451	OBD 01	129.55	130.05	gt-opx-plag-bi-opaque-cpx
R1643452	OBD 01	139.2	139.8	gt-opx-plag-bi-opaque-cpx
R1643453	OBD 01	123.7	123.85	gt-opx-plag-bi-opaque-cpx (sample altered)
R1643454	OBD 01	126.7	126.9	gt-hbd-plag-qtz-bi-opaque-minor cpx
R1643455	OBD 01	133.3	133.65	gt-hbd-cpx-plag-qtz-opaque-opx
R1643456	OBD 01	135.1	135.3	gt-opx-hbd-opaque-cpx-qtz
R1643457	OBD 01	135.9	136.1	gt-opx-hbd-opaque-cpx-qtz
R1643445	OBD 03	155.15	155.55	plag-qtz-bi(altered)-hbd(mostly altered)-opaque
R1643446	OBD 03	161.05	161.6	
R1643447	OBD 03	166.35	166.7	igneous plag-qtz-kspar-bi(altered)-hbd(mostly altered)-opaque-nice titanite coronas
R1643448	OBD 03	173.3	173.55	plag-qtz-hbd (altered)
R1643449	OBD 03	176.1	176.3	
R1643450	OBD 03	199.15	199.7	gt-bi (altered)-qtz-plag-opaque-K-spar
R1643444	OBD 05	132.1	132.5	K-spar-qtz-plag-hbd (altered) - minor gt-bi altered
R1643393	OBD 06	248	248.4	gt-bi-qtz-plag-K-spar
R1643394	OBD 06	250	250.25	bt-bi-qtz-plag -gt partially replaced by bi-plag)
R1643395	OBD 06	245	245.2	gt-bi-plag-K-spar-qtz
R1643396	OBD 06	246.3	246.65	gt-plag-qtz leucosome with enclosing gt-bi-qtz-plag
R1643397	OBD 07	261.65	262.65	k-spar-plag-bi-qtz
R1643398	OBD 07	264.4	264.75	bi-plag-qtz-K-spar relic gt (partially replaced by bi-plag)
R1643399	OBD 07	269.4	269.9	bi-plag-qtz-K-spar relic gt (partially replaced by bi-plag)
R1643400	OBD 08	175.25	175.84	bi-plag-qtz-opaque
R1643401	OBD 08	180	180.4	igneous K-spar-qtz-plag-bi-hbd (altered)
R1643402	OBD 08	183.1	183.6	igneous K-spar-qtz-plag-bi-hbd (altered)
R1643403	OBD 09	389.3	389.8	gt-bi-qtz-crd (altered)-K-spar
R1643404	OBD 09	392.3	392.7	gt-bi-plag-qtz-K-spar
R1643405	OBD 09	396.1	396.5	gt-bi-plag-qtz-K-spar
R1643391	OBD 11	227.7	228.15	hbd-plag-bi-qtz-opaque
R1643392	OBD 11	228.55	228.85	hbd-plag-bi-qtz-opaque
R1643412	OBD 12	467.65	468	gt-bi-plag-qtz-hbd (mostly altered)
R1643413	OBD 12	472.5	473.15	gt-bi-plag-qtz
R1643441	Lake Maurice East 1	731	731.2	mylonitic gt-qtz-K-spar--plag-opaque-(extensive alteration)
R1643442	Lake Maurice East 1	737.7	737.85	mylonitic gt-qtz-K-spar-opaque-sill-opx? (most are altered)
R1643443	Lake Maurice East 1	738.15	738.35	mylonitic gt-qtz-K-spar-opaque-minor sill
R1643409	Mt. Furner 1	551	551.33	gt-sill-bi-plag-qtz-late mus
R1643410	Mt. Furner 1	553.21	553.52	gt-sill-bi-qtz-mus (late)
R1643411	Mt. Furner 1	552.1	552.5	gt-minor sill-bi-plag-qtz-late mus

Sample No.	Drill hole name	Interval (m) From	To	Petrography of selected slides
R1643406	Manya 4	798.4	798.8	gt-bi-K-spar-qtz-plag
R1643407	Manya 4	800.1	800.5	gt-bi-plag-K-spar-qtz
R1643408	Manya 4	801.8	802.2	gt-bi-qtz-K-spar-partly alterd plag
R1643414	Middle Bore 1	422.15	422.37	
R1643415	Middle Bore 1	434.09	434.2	
R1643416	Middle Bore 1	438.85	439.1	
R1643417	Middle Bore 1	450.76	450.96	
R1643418	Middle Bore 1	459.07	459.23	
R1643419	Middle Bore 1	462.75	462.88	
R1643420	Middle Bore 1	479.9	480.1	gt-bi-plag-qtz-hbd (very altered)
R1643421	Middle Bore 1	489.1	489.25	
R1643422	Middle Bore 1	492.1	492.25	gt-qtz-plag-opx-bi-cpx (completely altered)
R1643423	Middle Bore 1	500.3	500.5	
R1643424	Middle Bore 1	502.2	502.35	
R1643425	Middle Bore 1	504.3	504.5	gt-hbd-plag (partly altered)-cpx (completely altered)-opaque-minor bi
R1643426	Middle Bore 1	506.3	506.5	
R1643427	Middle Bore 1	512.1	512.3	
R1643428	Middle Bore 1	512.4	512.6	plag-cpx (very altered-small relics)-qtz
R1643429	Middle Bore 1	517.3	517.6	plag-qtz-hbd-bi-opaque (moderate alteration)
R1643430	Middle Bore 1	519.2	519.4	
R1643431	Middle Bore 1	544.1	544.3	
R1643432	Middle Bore 1	466.4	466.62	
R1643433	Middle Bore 1	479.1	479.4	gt-plag-qtz-bi-opqaue-cpx (altered)
R1643434	Middle Bore 1	478.05	478.3	
R1643435	Middle Bore 1	480.5	480.7	
R1643436	Middle Bore 1	490.5	490.75	
R1643437	Middle Bore 1	492.6	492.85	
R1643438	Middle Bore 1	493.4	493.65	gt-plag-qtz-opaque-cpx-hbd
R1643439	Middle Bore 1	515.3	515.55	
R1643440	Middle Bore 1	555.1	555.25	
R1643458	Middle Bore 1	449.9	450.2	cpx-hbd-bi (ultramafic)